



Calhoun: The NPS Institutional Archive

Theses and Dissertations

Thesis Collection

1960-05

A preliminary evaluation of the Navion as a
lateral-directional flight simulator for use in the
investigation of flying qualities criteria

Ebbert, E. L.

Princeton University



Calhoun is a project of the Dudley Knox Library at NPS, furthering the precepts and goals of open government and government transparency. All information contained herein has been approved for release by the NPS Public Affairs Officer.

**Dudley Knox Library / Naval Postgraduate School
411 Dyer Road / 1 University Circle
Monterey, California USA 93943**

<http://www.nps.edu/library>

NPS ARCHIVE
1960.06
EBBERT, E.

A PRELIMINARY EVALUATION OF THE NAVION
AS A LATERAL-DIRECTIONAL FLIGHT SIMULATOR
FOR USE IN THE INVESTIGATION OF
FLYING QUALITIES CRITERIA

E. L. EBBERT
and
J. F. O'HARA

DUDLEY KNOX LIBRARY
NAVAL POSTGRADUATE SCHOOL
MONTEREY CA 93943-5101

A PRELIMINARY EVALUATION OF THE NAVION
AS A LATERAL-DIRECTIONAL FLIGHT SIMULATOR
FOR USE IN THE INVESTIGATION OF
FLYING QUALITIES CRITERIA

E. L. Ebbert, Lieutenant, USN
J. F. O'Hara, Lieutenant, USN

Aeronautical Engineering Report No. 509

May 1960

Submitted in partial fulfillment of the requirements for the
degree of Master of Science in Engineering from Princeton
University, June, 1960

NPS ARCHIVE

1960.06

EBBERTE, E.

~~CONFIDENTIAL~~
~~SECRET~~

CONFIDENTIAL
EXCLUDED FROM AUTOMATIC
DOWNGRADING AND
DECLASSIFICATION

ACKNOWLEDGEMENTS

The authors wish to express their appreciation to Professors Edward Seckel and Dunstan Graham, of the Princeton University Aeronautical Engineering faculty, for their assistance and guidance throughout the conduct of this investigation.

Appreciation is also expressed to Mr. Enoch Durbin, Mr. Theodor Dukes and the technical staff of the Flight Mechanics Department whose assistance in the design, installation, and maintenance of the autopilot system proved invaluable.

A PRELIMINARY EVALUATION OF THE NAVION
AS A LATERAL-DIRECTIONAL FLIGHT SIMULATOR
FOR USE IN THE INVESTIGATION OF
FLYING QUALITIES CRITERIA

SUMMARY

A preliminary evaluation was made of a modified North American Navion airplane for use as a lateral-directional flight simulator in the investigation of flying qualities criteria. Modification of the test airplane was accomplished by installation of a three axis, variable feedback autopilot and associated controls and sensing transducers. An analytical development, based on servo-analysis methods, suggested the ratio of the numerator and denominator frequency terms in the roll angle to aileron control deflection transfer function as a possible flying qualities criterion. This parameter was suggested by I. L. Ashkenas and D. T. McRuer whose analytical work provided the basis for parts of this investigation. A limited flight test program was conducted to evaluate the simulation capabilities of the modified NAVion and to make a preliminary investigation of the proposed flying qualities criterion.

The modified NAVion was found to be capable of simulation of the lateral-directional modes of motion over a considerable range and to be of some utility for pilot-opinion investigation of flying qualities criteria. The flight test results indicated the possibility that the proposed flying qualities criterion may be a valid one, provided assigned numerical limits are functions of anticipated roll rates.

Recommendations were made, where applicable, for correction of deficiencies found in the variable feedback autopilot system.

The investigation was conducted at the Forrestal Research Center, Princeton University, during the 1959-1960 academic year.

TABLE OF CONTENTS

	page
Summary	i
List of Tables	iv
List of Figures	v
Symbols and Definitions	vii
Section I - Introduction	
Section II - Equipment	2
Test Airplane	2
Autopilot	3
Instrumentation	7
Calibration	8
Ground Station	11
Analog Computer	12
Section III - Discussion	13
Equations of Motion	20
Simulation of an Arbitrary "X" Airplane	24
Analog Computer Study	27
Flight Phase	31
Section IV - Conclusions	38
Tables	
Figures	
References	
Appendix A	A-1
Numerical Evaluation of Gain Constants	
For Simulation of the "X" Airplane	

TABLES

I	Physical Characteristics of the NAVion
II	Physical Characteristics of Instrumentation Components
III	Defining Equations for Equivalent and Artificial Stability Derivatives
IV	Numerical Solutions for Feedback Gain Constants
V	Numerical Values for Basic NAVion Stability Derivatives
VI	Analog Computer Equations and Potentiometer Settings
VII	Analog and Flight Test Results

FIGURES

TEST AIRPLANE CONFIGURATION

1. Photograph of Test Airplane
2. Autopilot Block Diagram - Yaw Channel
3. Autopilot Block Diagram - Roll Channel
4. Photograph of Gain Potentiometer Panel
5. Photograph of Equipment Compartment - Top View
6. Photograph of Equipment Compartment - Stern View
7. Autopilot Summing Circuit - Yaw Channel and Main Terminal
Strip Numbering System
8. Autopilot Summing Circuit - Roll Channel
9. Photograph of Cockpit Configuration
10. Deleted
11. Photograph of Angle-of-attack and Sideslip Vane Boom

CALIBRATION CURVES

12. K_4 , DEG Rudder Per DEG β
13. K_8 , DEG Aileron Per DEG β
14. K_6 , DEG Rudder Per DEG/SEC $\dot{\psi}$
15. K_{10} , DEG Aileron Per DEG/SEC $\dot{\psi}$
16. K_5 , DEG Rudder Per DEG/SEC $\dot{\phi}$
17. K_9 , DEG Aileron Per DEG/SEC $\dot{\phi}$
18. K_{11} , DEG Aileron Per DEG ϕ
19. DEG Rudder Per Volt Versus Ratio Adjustment Setting
20. Telemeter Calibration
21. Lateral-Directional Analog Circuitry - Basic NAVION
22. Rudder and Aileron Analog Circuitry - "X" Airplane

FIGURES (continued)

ANALOG AND FLIGHT TEST RESULTS

23. Basic Airplane - Response to Step Aileron Deflection

24. "X" Airplane - Response to Step Aileron Deflection

25. "X" Airplane - Response to Step Aileron Deflection for

$$\zeta_x = 0.915 \text{ and } \zeta_r = 0.383$$

26. "X" Airplane - Response to Step Aileron Deflection for

$$\zeta_x = - .0492 \text{ and } \zeta_r = - .542$$

27. Dutch Roll Response - Basic Airplane and "X" Airplane

SYMBOLS AND DEFINITIONS

SYMBOLS

β	Sideslip angle
δ_A	Aileron deflection due to lateral stick displacement
δ_R	Rudder deflection due to rudder pedal displacement
δ_X	Rudder deflection due to lateral stick displacement
δ_a	Total aileron deflection
δ_c	Equivalent aileron deflection for a general roll-control system
δ_n	Total rudder deflection
Δ	Lateral-directional characteristic equation
\mathcal{P}_d	Dutch roll damping factor
\mathcal{P}_ϕ	Numerator damping factor in roll angle to aileron deflection transfer function
$\Theta_{\phi\phi}$	Roll channel servo-drum rotation
$\Theta_{\phi\psi}$	Yaw channel servo-drum rotation
ϕ	Roll angle
$\dot{\phi}$	Roll rate
$\dot{\psi}$	Yaw rate
ω_d	Dutch roll undamped natural frequency
ω_ϕ	Numerator undamped natural frequency in roll angle to aileron deflection transfer function
e	Naperian log base
g	Acceleration of gravity, feet per second ²

SYMBOLS AND DEFINITIONS (continued)

h_p	Pressure altitude, feet
$ p_1 $	Magnitude of first overshoot of roll rate response from steady-state roll rate after an aileron-step input
p_{ss}	Steady state roll rate
A_ϕ	Coefficient of roll angle to aileron deflection transfer function
$C_{1/2}$	Cycles to damp to half amplitude
I_{xz}	Cross product of inertia, slug-feet ²
K_i	Feedback gain factor, (0-1)
p_1	Potentiometer setting
$\frac{1}{T_R}$	Rolling convergence root of the lateral-directional characteristic equation
$\frac{1}{T_S}$	Spiral root of the lateral-directional characteristic equation
U_0	Velocity, initial conditions, feet per second
L_p	$\frac{C_{lp}}{2J_x T}$
L_r	$\frac{C_{lr}}{2J_x T}$
L_β	$\frac{\mu C_{l\beta}}{J_x T^2}$
L_{δ_c}	$\frac{\mu C_{l\delta_c}}{J_x T^2}$
L_{δ_r}	$\frac{\mu C_{l\delta_r}}{J_x T^2}$
L_ϕ	Artificial derivative, rolling moment due to roll angle
N_p	$\frac{C_{np}}{2J_z T}$
N_r	$\frac{C_{nr}}{2J_z T}$

SYMBOLS AND DEFINITIONS (continued)

N_{β}	$\frac{\mu C_{n\beta}}{J_z \tau^2}$	
N_{δ_c}	$\frac{\mu C_{n\delta_c}}{J_z \tau^2}$	
N_{δ_n}	$\frac{\mu C_{n\delta_n}}{J_z \tau^2}$	
N_{ϕ}		Artificial derivative, yawing moment due to roll angle
Y_p	$\frac{b}{4\tau} C_{yp}$	
Y_r	$\frac{b}{4\tau} C_{yn}$	
Y_v	$\frac{1}{2\tau} C_{y\beta}$	

DEFINITIONS

Double-primed derivatives indicate "equivalent or artificial stability derivatives."

Aileron deflection is defined as the sum of the magnitudes of angular deflection of the right and left ailerons, positive to give positive rolling moments.

Gain Potentiometer - A potentiometer controlling the gain of a feedback signal from a sensor-transducer or a signal from one of the electrical flight controls.

Ratio Adjustment - A potentiometer controlling the gain of a servo-drum position feedback signal.

The non-dimensional derivative symbols used are defined in Ref. 5. All other symbols are defined as used.

SECTION I

INTRODUCTION

The lateral-directional flying qualities criteria as reflected in current military specifications are suspected of being inadequate for modern high-performance manned aircraft. The possibility is suggested that aircraft capable of high speed, high altitude operations may satisfy all of the current specifications and still not be acceptable to the pilot for the successful accomplishment of all his assigned missions. It is also noted that some current aircraft do not satisfy published specifications and have been accepted only after exceptions to the specifications have been approved. The addition of complex automatic control systems is often required to attain acceptable handling qualities.

The task of obtaining suitable parameters which correlate pilot opinion with the measurable or predictable lateral-directional stability and control characteristics is, in general, very complex. This general problem has been the subject of many investigations. Extensive use has been made of ground simulators and variable stability aircraft in order to formulate these parameters in terms of data obtained from the lateral-directional motion time histories. The selected parameters should be related to the aerodynamic stability derivatives over which the aircraft designer has some measure of control. Such parameters, if valid, could be used in the design phase in order to predict and improve flying qualities of a proposed aircraft.

One approach to this problem has been advanced which has as a general objective the simplification of the automatic control and stability augmentation devices necessary for acceptable vehicle performance. This approach considers airframe, control system and pilot as the three elements of a closed-loop servo system in order to improve the compatibility of the individual elements and optimize the over-all performance. Using servo-analysis techniques, the combined system response is predicted. The transfer functions of the airframe element must necessarily contain the stability derivatives over which the designer has some control. The design problem is then the integrated problem of designing to meet both the performance and the handling qualities specifications. Where compromises are necessary, the designer may choose to use automatic control system elements to provide over-all satisfactory performance of the system. From this approach a set of parameters have been defined, some of which are not contained in the military handling qualities specifications, but which have been suggested as important handling qualities criteria.

The purpose of this investigation is to determine the feasibility of using the NAVion class airplane in the simulation of an arbitrary airplane, and to study the response of the simulated airplane to the variation of one of the proposed lateral-directional handling qualities criteria derived from the combined system approach.

For this purpose, a three-axis variable feedback autopilot was installed in a NAVion airplane, and a series of flight experiments was performed to evaluate the system.

SECTION II

EQUIPMENT

The variable stability flight simulator used in this investigation was a North American NAVion airplane. To provide the variable stability capability, a modified Minneapolis-Honeywell autopilot, USAF Type E-12, was installed. The modification of the autopilot consisted of addition of supplementary rate gyros, sideslip and angle of attack transducers and an airspeed transducer. Signals from the transducers, proportional to the measured quantities, were introduced as input signals to the autopilot, resulting in control deflection proportional to the measured quantity. This made the system capable of effectively modifying the airplane stability derivatives. Data collection and recording were accomplished by means of an ASCOP pulse width/frequency modulated telemetering system. An analog computer, GEDA, was used in the theoretical development of the problem.

TEST AIRPLANE

The NAVion is an all metal, low wing, four place airplane powered by a single engine. The engine, a Continental E-185, drives a variable pitch Hartzel propeller and is rated to deliver 185 horsepower for maximum continuous power at sea level at 2300 RPM. The control surfaces are of conventional design. The ailerons, frise type, have a streamlined static balance fixed at the outboard end of each aileron. The trim tabs for the aileron and rudder are of the fixed-bend type, and the elevator trim tab is adjustable from the cockpit. The physical characteristics of the NAVion are listed in Table I. A photograph of the test airplane

is shown in Fig. 1. The airplane was modified for this investigation by the installation of a three-axis variable feedback autopilot.

AUTOPILOT

The basic autopilot, designed for use in a Piasecki H-21 helicopter, controls and alters stability of the airplane in the pitch, roll and yaw axes through three channels of operation. Each channel is composed of an AC series summing network which combines signal voltages from the sensing transducers, the electrical flight controls and the knob actuated trim controller. The difference between this combined signal voltage and a voltage feedback signal from the servo-drum position transducer, an error signal, is applied to an amplifier, phase discriminated and transferred into servo drum rotation by means of dual power relays. The servo drum rotation moves the control surfaces through the conventional cable control system of the aircraft. The motion of the control surface continues until error signal voltage at the input to the amplifier is reduced to a value below the threshold of the system. This value is about fifty millivolts.

The suitability of using this autopilot in the NAVion airplane to provide equivalent (artificial or variable) stability derivatives was verified from a single sensor control loop system study using servo-analysis methods. The control loop containing the servo positioning loop, the airframe, and a rate gyro was synthesized. Assuming the system to be linear, the transfer functions of the system elements were estimated for each channel. The open and closed loop amplitude and phase characteristics were determined using Bode diagrams. The analysis showed the

response of the autopilot system to be too slow to control the longitudinal short period motions of the aircraft. This necessitated the installation of a larger drum on the pitch channel servo-motor. To assure that the closed loop attenuation of the autopilot response to a gyro oscillation at the rate gyro natural frequency, estimated to be four cycles per second, would be sufficient to prevent instability of the system, the natural frequency of the rate gyros was increased to about eight cycles per second. This was accomplished by clipping off eight turns of each centering spring in each rate gyro.

The basic autopilot was modified by deleting some of the original provisions and by supplying additional feedback loops. The directional coupler feedback loop, the flight control stick trim provisions, and the coordinated turn provisions were eliminated. Sideslip angle and roll rate feedback loops and a cross-control signal proportional to aileron control stick deflection were added to the yaw channel. Sideslip angle and yaw rate feedback loops were added to the roll channel. Block diagrams of the modified yaw and roll channels are shown in Figs. 2 and 3. The manually adjustable ratio potentiometers were relocated on a gain control panel placed between the pilots' seats as shown in Fig. 4. An electronic safety device was installed to prevent "hard-over" signals by automatically disengaging the autopilot if an error voltage exceeding approximately 3 volts should instantaneously appear at the amplifier input. The nature of the AC summing networks was such that signals from any one of the transducers could be fed into two channels. If an additional sensed quantity was required for two channels, a separate potentiometer input was necessary.

An auxiliary circuit was placed in the aileron control summing network which allowed the pilot to select any desired step input of voltage, simulating a control deflection step input.

The installation of the autopilot components and instrumentation of the test airplane was done in conjunction with another research group. The mechanical installation of the servo-motor units, the tie-in with the NAVION control system and the external instrumentation booms are described in Ref. 1. The installation of the electrical components and the cockpit modification are described in subsequent paragraphs.

The servo-motor units were mounted on a fuselage frame aft of the equipment compartment. The cable connection between the servo-drums and the airplane control cables was accomplished through pulley systems.

The electrical components of the autopilot were installed on a metal equipment table located in the equipment compartment. The general arrangement of components of the system is shown in Figs. 5 and 6. Electrical cabling from the transducers, and from the stick and knob actuated flight controllers was joined with the cabling to the servo units and the calibration unit through a terminal board. This board facilitated the wiring and trouble-shooting, and provided flexibility in configuration changes. The schematic wiring diagrams of the AC summing circuits are shown in Figs. 7 and 8. The excitation voltages for the transducers were provided by four multiple-wound sealed transformer units located on the equipment table. The polarity of each feedback quantity could be changed by reversing the transducer potentiometer excitation voltage leads on the main terminal board. The power for the autopilot system was provided from the 28 volt DC aircraft system and a regulated 400 cycle, 115 volt, single phase AC inverter.

The co-pilot's cockpit area was modified to provide for the stick and knob actuated flight controllers, the electrical rudder pedals and the gain control panel. The general arrangement of the cockpit is shown in Fig. 9. The rudder pedal configuration was designed so that the travel of the pedals was approximately the same as those of the basic NAVion. The pedals were spring loaded to the center position and operated a 360 deg. potentiometer, located under the stick flight controller, through a cable and pulley system. The co-pilot's seat track was extended to allow further aft adjustment of the seat in order to provide ample room for the test pilot to manipulate the controls. Dis-engage switches were provided on the pistol grip stick controller and for the safety pilot on the left console. The force-feel system for the controls consisted of the springs on the rudder pedals and a spring centered stick flight controller with an adjustable fluid damper. The stick flight controller requires a small break-out force to deflect the stick from the centered position. Since this characteristic was not considered objectionable, the controller was not modified.

Quantities to be telemetered were taken from the appropriate terminals on the main terminal board to a 15 channel filter-conversion unit which converted the voltage to DC. The terminal numbers associated with the various elements of the summing circuits are shown in Figs. 7 and 8. The terminal numbering scheme for the main terminal board is shown in Fig. 7.. A gain control for each channel permitted the DC voltage to be adjusted to that required by the telemetering system (0-5 volts). From the filter-conversion unit, the DC voltages representing the measured

quantities were taken to an auxiliary terminal strip and connected to the telemeter transmitter unit.

Ground adjustments of the complete autopilot system included:

- (1) setting the control system cable tension to 30 lbs.;
- (2) setting the servo unit over-ride clutches for the proper output torque so that the safety pilot could over-ride the servo motors when the autopilot was engaged;
- (3) setting the limit switches in the servo unit to interrupt power to the servo motor at a drum angular position less than that required to drive the control surface to the mechanical control stops;
- (4) setting the amplifier sensitivity and throttling controls;
- (5) removing the quadrature voltage; and
- (6) fully calibrating the system.

INSTRUMENTATION

The transducers in the feedback loops of the modified autopilot provided signals to the autopilot amplifier through the AC summing networks and provided the signals required to measure the aircraft motions. The flight condition data (airspeed, altitude, and outside air temperature) were obtained from standard aircraft instruments. Errors in these instruments were assumed negligible. The physical characteristics of the components of the instrumentation system are listed in Table II.

Two of the modified rate gyros were located on the autopilot chassis on the main equipment table and two were mounted on the floor of the aircraft in the equipment compartment as shown in Fig. 5.

The pitch-roll attitude gyro was mounted on the main equipment table on the autopilot chassis as shown in Fig. 6.

The use of a single sideslip vane was possible because it contained two separate potentiometers. The sideslip vane was installed on a boom extending four feet ahead of the wing leading edge at the wing tip. It was assumed that this distance was adequate to minimize measurement errors due to the wing pressure field. The vane configuration is shown in Fig. 11. The position of the sideslip vane was such that the yawing rate of the aircraft about the vertical body axis would affect the sideslip angle measurement slightly, but this effect was neglected.

The telemeter transmitter unit consists of a rotary switch sampling each of 43 input channels plus two synchronizing channels at the rate of 20 times per second. The sampled data are converted to pulse width form by a keyer unit and transmitted as a UHF frequency modulated signal to the telemeter ground station. The filter-conversion unit limited the data measurements to 14 quantities plus a full scale reference voltage. By jumper wiring on the auxiliary telemetering terminal strip it was possible to sample a given quantity more than once for each revolution of the switch. Specifications of the telemeter transmitter unit are listed in Table II.

CALIBRATION

The purpose of the system calibration was twofold:

- (1) to obtain data which would give the desired feedback gain potentiometer setting to produce a given value of the equivalent stability derivative. The gain setting produces a ratio of the units of control deflection per unit of the quantity measured.

- (2) To obtain data required to convert the received telemeter signals at the ground station into equivalent measured flight data.

The feedback gain potentiometer setting data were obtained by measuring and plotting:

- (1) the transducer output voltage versus the magnitude of the measured quantity;
- (2) the corrected gain potentiometer settings; (This was necessary because the potentiometers used had two linear ranges, and required the determination of the face-plate settings for any given output to input ratio);
- (3) the control deflection per voltage input to the amplifier for a given ratio adjustment of the servo-position feedback loop.

Since the excitation voltage of the gain potentiometer was supplied by the output of the corresponding transducer, the product of these parameters gave the control deflection per unit of measured quantity as a function of the potentiometer face-plate setting.

$$\frac{\text{voltage output}}{\text{unit measured quantity}} \times \text{corrected potentiometer setting} \times \frac{\text{control deflection}}{\text{voltage input to AP}} \\ = \frac{\text{control deflection}}{\text{unit measured quantity}}$$

The rate gyros were calibrated by placing the gyro on a turntable, exciting the gyro from the aircraft circuitry and measuring the output voltage for various timed rotation rates of the turntable.

The roll angle gyro was calibrated at zero and plus or minus ten degrees of roll angle by tilting the gyro case with a measured ten degree wedge and measuring the output voltage.

The sideslip vane potentiometers were calibrated by measuring output voltage versus sideslip angle by means of a protractor mounted on the vane.

The gain potentiometer face-plate setting versus the ratio of output voltage to input voltage was obtained by exciting the potentiometer with a known voltage and measuring the output voltage as a function of the potentiometer setting. "Face-plate setting" is emphasized because the true zero positions of the potentiometers did not correspond with zero face-plate readings in all cases. No appreciable loading effects were noted.

The control deflection versus voltage input to the servo-position control loop was obtained by measuring control deflection for various input voltages. Rudder angle was measured with a calibration protractor mounted on the vertical stabilizer. Aileron deflection was considered as the sum of the magnitudes of the angular deflections of the two ailerons. Angular deflection was measured with a protractor attached to the aileron static balance-weight arm. Aileron calibration was made for the roll position servo ratio adjustment at a maximum setting (minimum degrees of drum rotation per volt), while the rudder calibration was made for the entire range of the yaw ratio adjustment.

The transducers were nearly linear throughout their useful range. Rudder and aileron deflection were linear with respect to input voltage for given servo control ratio adjustments. The departures from linearity were in the control deflection per unit input voltage versus the position servo control ratio adjustment, and the feedback gain potentiometers. The latter were special purpose potentiometers which were approximately linear from zero to about seven tenths total wiper travel, at which point the

output was 96% of the excitation voltage. The response in the last three tenths wiper travel was linear but with a large slope change due to a larger size wire in the potentiometer winding.

The calibration data for the gain potentiometer settings versus the control deflection per unit measured quantity, and versus transducer voltage output per unit measured quantity are shown in Figs. 12 through 19.

The data required to convert the telemetered data into equivalent flight data involved the calibration of the filter-conversion unit. The AC voltage input was measured and plotted versus the DC voltage output. The AC voltage input corresponded to the AC voltage output of the appropriate sensing transducer, previously calibrated, with a linear shift of the zero reference. Calibration data showing percentage full-scale (0-5 volts DC) versus magnitude of the measured quantities are shown in Fig. 20.

GROUND STATION

The ground station data collection equipment consisted of an ASCOP M series PW/FM ground station, an Ampex Model 309C dual track tape recorder and associated graphical recorders.

The ASCOP ground station received the modulated signals from the airborne unit, demodulated and decoded the signals to provide for each of the 43 channels of information, and provided a continuous voltage output to the recorders representing the measured flight data.

The tape recorder had provisions for simultaneous recording of telemeter and voice transmissions. This permitted the recording of description of runs, pilot's comments and ground station operator's comments along with the telemeter data.

Sanborn four channel pen recorders, Model 154-100B, were used in the graphical recording phases.

ANALOG COMPUTER

The analog computer used in this investigation was a Goodyear Aircraft Corporation Model L3 (GEDA) linear electronic differential analyzer. Twenty-four automatically stabilized DC computing amplifiers were available with open-loop gain greater than 5×10^7 , and of negligible drift. The computer incorporated an automatic error indicator and had a guaranteed accuracy of one percent. Provisions were available for accurately setting computer board potentiometers by the use of a special calibration potentiometer and null indicator.

SECTION III

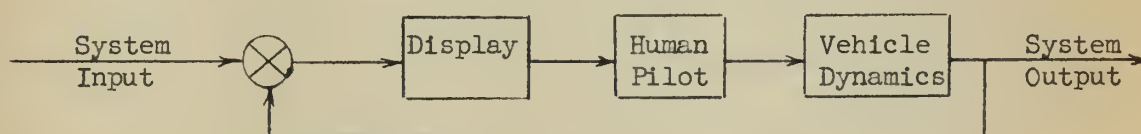
DISCUSSION

The development and meaning of a proposed lateral-directional flight acceptability criterion is briefly described in this section. It was not within the scope of this investigation to conduct a complete pilot-opinion study, but only to outline such a study from an analytical point of view and to confine the experimental phase to the preliminary evaluation of the modified NAVion as a possible research vehicle for a more extensive and complete study.

The particular aspect of the lateral-directional response under consideration in this investigation is the roll rate response to aileron deflection. Although aileron deflection is referred to frequently in the subsequent discussion, the analysis would apply equally well to a spoiler or other type of roll control system. The roll rate response is of considerable importance to the military pilot in that a high degree of precision in roll control is required for the maneuvering and "closed-loop" tracking phases of many tactical missions. From the pilot's viewpoint it would be desirable to have roll rate directly proportional to control deflection with no time lag and no induced transient oscillation. Flying qualities parameters which could measure the departure of the roll response from this idealized condition would then be very desirable. In addition, any such parameter should be simply expressible in terms of aircraft stability derivatives and should correctly reflect pilot opinion in terms of measurable quantities from time histories of the lateral-directional dynamic response.

The airframe designer might then interpret such "valid" flying qualities criteria in terms of stability derivatives and thereby increase the predictability of satisfactory dynamic performance from the vehicle without the necessity for extensive modifications of the completed airplane by later addition of complex stability and control augmentation devices.

A combined system approach using servo-analysis techniques considers the airframe, the pilot and the control system as elements of a closed loop servo system. The block diagram of such a system is indicated in the following illustration:



The transfer functions of the airframe, the control system, and the human describing function are known to at least a first order approximation, and the system performance may be evaluated using conventional servo-analysis techniques. From this analytical approach, described in detail in Ref. 2, a set of possible flying qualities criteria are defined. Their relationships to the human pilot describing function, and to the lateral-directional airframe transfer functions, are indicated. Using available experimental data and approximate airplane transfer functions in terms of stability derivatives, numerical ranges for the proposed set of parameters were defined which represent a "good" equivalent airframe. These proposed flying qualities criteria were compared with the current military specifications and with the results of a large number of flying quality experiments. The

conclusion was drawn that the parameter $\frac{\omega_\phi}{\omega_d}$, the ratio of the numerator to the denominator frequency terms in the roll angle to aileron control deflection transfer function, $\frac{\phi}{\delta_a}$, might provide a useful and important specification. This parameter is not explicitly contained in the military specifications.

This ratio, $\frac{\omega_\phi}{\omega_d}$, is approximated by:

$$(1) \left(\frac{\omega_\phi}{\omega_d} \right) \doteq 1 - \frac{L\beta N\delta_c}{N\beta L\delta_c}$$

The parameter is derived from the $\frac{\phi}{\delta_a}$, transfer function which in Laplace notation is represented as:

$$(2) \frac{\phi(s)}{\delta_a(s)} = \frac{N_\phi(s)}{\Delta(s)} = \frac{A_\phi (s^2 + 2\zeta_\phi \omega_\phi s + \omega_\phi^2)}{(s \pm \frac{1}{T_S})(s + \frac{1}{T_R})(s^2 + 2\zeta_d \omega_d s + \omega_d^2)}$$

The denominator is the lateral-directional characteristic equation showing the conventional factorization which is the spiral, the rolling mode, and the dutch roll roots, respectively. The numerator is obtained from the Cramer's rule solution of the lateral-directional simultaneous differential equations of motion for the roll angle. If the control input is a unit step aileron deflection, the rolling velocity transform is:

$$(3) \dot{\phi}(s) = \frac{A_\phi (s^2 + 2\zeta_\phi \omega_\phi s + \omega_\phi^2)}{(s \pm \frac{1}{T_S})(s + \frac{1}{T_R})(s^2 + 2\zeta_d \omega_d s + \omega_d^2)}$$

where the coefficients in terms of stability derivatives are approximated by:

$$A_\phi = L\delta_a$$

$$\omega_\phi^2 \doteq N_\beta \left(1 - \frac{L\beta N\delta_c}{N\beta L\delta_c} \right)$$

$$2\zeta_\phi \omega_\phi \doteq -(\gamma_v + N_r) + \frac{N\delta_a L_n}{L\delta_a}$$

$$\omega_d^2 \doteq N_\beta$$

$$2\zeta_d \omega_d \doteq -(\gamma_v + N_r) - \frac{L\beta}{N_\beta} \left(N_p - \frac{g}{U_0} \right)$$

$$\frac{1}{T_R} \doteq -L_p + \frac{L\beta}{N_\beta} \left(N_p - \frac{g}{U_0} \right)$$

$$\left| \frac{1}{T_S} \right| \doteq \left| T_R \frac{g}{U_0} \left(\frac{L\beta}{N_\beta} N_r - L_n \right) \right|$$

In the preceding approximations the product of inertia, I_{xz} , has been neglected, and these approximations are subject to validity conditions, defined in Appendix A.

From the representation of Equation (3) in terms of the stability derivatives, the similarity of the second order terms is apparent. In particular, for the case where the second order factors are equal, and the spiral root is small, the rolling velocity equation reduces to the single degree of freedom rolling equation. This condition occurs when:

$$\begin{aligned} 2 \zeta_d \omega_d &= 2 \zeta_\phi \omega_\phi \\ \omega_d &= \omega_\phi \end{aligned}$$

Assuming this condition initially, the departure of the ratio $\frac{\omega_\phi}{\omega_d}$ from unity will indicate the magnitude of the induced dutch roll oscillation about the steady state roll rate response of an airplane to an aileron control deflection. The damping ratio terms are normally of the same order. The effect of the departure of the ratio $\frac{\omega_\phi}{\omega_d}$ from unity is clearly illustrated by the relative pole-zero locations on root-locus diagrams of the $\frac{\phi}{\delta a}$ transfer function.

By further assuming that the damping ratios are small and that the spiral root is small, an approximate inverse transform of Equation (3) may be written as:

$$(4) \frac{\dot{\phi}(t)}{T_R L \delta_a \delta_a} = \left(\frac{\omega_\phi}{\omega_d}\right)^2 e^{\pm \frac{t}{T_S}} - \frac{1 + \omega_\phi^2 T_R^2}{1 + \omega_d^2 T_R^2} e^{\pm \frac{t}{T_R}} + \frac{\left(\frac{\omega_\phi}{\omega_d}\right)^2 - 1}{1 + \omega_d^2 T_R^2} e^{-s_d \omega_d t} \sin\left(\omega_d t - \sin^{-1} \frac{1}{\sqrt{1 + T_R^2 \omega_d^2}}\right)$$

where the terms indentify, in order, the rolling motion associated with the spiral, roll subsidence and dutch roll modes.

If Equation (4) represents a valid approximation of the rolling velocity response to a step aileron input, then the influence of the parameter $\frac{\omega_\phi}{\omega_d}$ and the effect of its departure from unity on the magnitude of the steady state and the dutch roll mode is clearly shown.

It is noted that an exact literal solution of the inverse transform without use of appropriate approximations is extremely complex, and because of its complexity is not too useful.

Equation (4) was presented by the authors of Ref. 2, and the extent of the approximations used in the derivation is not known. Even if the approximations are basic, the usefulness of Equation (4) is not destroyed, in that it may be used to analyze the roll response and to calculate approximate solutions for specific examples. If the validity of the equation is in doubt for a particular application, recourse to more exact solutions from digital or analog computers would provide accurate and rapid information concerning the nature of the roll response.

In order to investigate the effect of the ratio $\frac{\omega_\phi}{\omega_d}$ on the roll response to an aileron step input, it was observed that the ratio could be changed by artificially varying the ratio $\frac{N \delta_c}{L \delta_c}$. Varying this ratio

for an airplane with a known characteristic equation would serve to maintain constant characteristic modes of motion and then pilot-opinion would be affected only by the variation of the ratio $\frac{\omega_\phi}{\omega_d}$.

For a pilot-opinion investigation, a measurable parameter which might be used to correlate pilot-opinion and the time history of the roll rate response to a step aileron input is the ratio of the magnitude of the first overshoot to the steady state rolling velocity, $\frac{|P_1|}{P_{ss}}$. This "correlation parameter" was used in a ground simulator pilot-opinion study described in Ref. 3. The test results indicated a good correlation between the parameter, $\frac{|P_1|}{P_{ss}}$, and pilot opinion. The conclusion was drawn that this was a valid parameter, and that the maximum acceptable value was 4.5%. This correlation parameter was defined in terms of stability derivatives as:

$$(5) \quad \frac{|P_1|}{P_{ss}} = \frac{|P_1|}{|B|} \omega_n \frac{L_p}{L\delta - \frac{L\beta N\delta}{N\beta}} \cdot \frac{N\delta}{N\beta} e^{-\frac{.347}{\zeta^{1/2}}}$$

This correlation parameter is equivalent to the ratio of the dutch roll magnitude to the steady state rolling velocity magnitude terms of Equation (4), which for the conventionally small spiral root may be written:

$$(6) \quad \frac{|P_{OR}|}{P_{ss}} = \frac{1 - (\frac{\omega_d}{\omega_\phi})^2}{\sqrt{1 + \omega_d^2 T_R^2}} e^{-\zeta_d \omega_d t} \sin(\omega_d t - A)$$

Equation (6) can be shown to be identical to Equation (5) by making the following substitutions:

$$\begin{aligned}
\text{phase angle} & A = -\frac{\pi}{2} \\
\text{time to first overshoot} & t_1 = \frac{\pi}{\omega_d} \\
\text{cycles to 1/2 amplitude} & C_{1/2} = \frac{\pi_{1/2}}{P} = \frac{.693}{2\pi\zeta} \\
\frac{|\Phi|}{|\beta|} & \doteq -\frac{L\beta}{N\delta} \left(\frac{1}{\sqrt{1 + \frac{1}{\omega_d^2 T_R^2}}} \right) ; \quad \frac{1}{T_R} \doteq -L\rho
\end{aligned}$$

The latter two substitutions are first order approximations. In addition, it is necessary to adopt the same sign convention for the aileron deflection used in the two equations.

One notes in Equations (4) and (6) that for values of $\frac{\omega_\phi}{\omega_d} = 1$ there will be no dutch roll magnitude nor any overshoot in the roll response to an aileron control deflection. This may occur when the derivative $N\delta$ is equal to or close to zero. The absence of an overshoot indicates a desirable rolling response, and for those cases where the $\frac{\omega_\phi}{\omega_d}$ ratio is close to one, then other parameters of the proposed set will specify satisfactory dutch roll oscillatory characteristics.

The fact that two completely independent investigations, one experimental and the other primarily analytical, result in the same suggested handling qualities parameter adds credence to the possibility that the ratio $\frac{\omega_\phi}{\omega_d}$ may prove to be an important criterion. In addition, the parameter $\frac{|\rho|}{\beta_s}$ provides a convenient way of measuring the $\frac{\omega_\phi}{\omega_d}$ ratio from flight test or analog data.

It is emphasized that in the foregoing development and discussion of the effects on the roll response for the case when the ratio $\frac{\omega_\phi}{\omega_d}$ differs from unity that there will be an associated effect on the quantity $2\zeta_\phi\omega_\phi$. It has been assumed that the condition:

$$2\zeta_\phi\omega_\phi = 2\zeta_d\omega_d$$

has not been altered significantly. For a particular case under examination, consideration must be given to the effects on the roll response and in particular on the magnitude of the dutch roll response due to deviations from this equality.

EQUATIONS OF MOTION

The NAVion airplane and the variable feedback autopilot were considered together as a linear "equivalent airframe" system, with the equivalent or artificial stability derivatives generated by the variable feedback loops and the associated control deflections. It was considered desirable to express the lateral-directional set of the small perturbation equations of motion in a dimensional form:

$$(7 - 1) \quad (S - Y_v)\beta + \dot{\psi} - \frac{g}{U_0} \phi = Y_{\delta_n} \delta_n$$

$$(7 - 2) \quad -L_{\beta} \beta - L_n \dot{\psi} + (s^2 - L_p s) \phi = L_{\delta_a} \delta_a + L_{\delta_n} \delta_n$$

$$(7 - 3) \quad -N_{\beta} \beta + (S - N_v) \dot{\psi} - N_p s \phi = N_{\delta_a} \delta_a + N_{\delta_n} \delta_n$$

These equations were obtained from Ref. 4, and differ from them by the following assumptions and change of variables.

$$\beta = \frac{v}{U_0} ; \quad N_v = \frac{N_{\beta}}{U_0} ; \quad L_v = \frac{L_{\beta}}{U_0} ; \quad p = \dot{\phi} ; \quad r = \dot{\psi}$$

$$Y_p \triangleq Y_n \triangleq Y_o \triangleq I_{xz} \triangleq N_v \triangleq Y_{\delta_a} \triangleq 0$$

The lateral control inputs may arise from any type of control system, but the conventional control system of the NAVion dictated the control notations δ_n and δ_a for conventional rudder and aileron control deflections.

An exact equivalence of Equation (7) and Equations (11-34) of Ref. 5 may be shown by expressing the latter in real time, in Laplace notation, and in the following form:

$$(8 - 1) \left(s - \frac{c_{y\beta}}{2\tau} \right) \beta + \dot{\psi} - \frac{c_{L_0}}{2\tau} \phi = \frac{c_{y\delta_n}}{2\tau} \delta_n$$

$$(8 - 2) - \frac{\mu c_{L\beta}}{J_x \tau^2} \beta - \frac{c_{L_n}}{2J_x \tau} \dot{\psi} + \left(s^2 - \frac{c_{Lp}}{2J_x \tau} s \right) \phi = \frac{\mu c_{L\delta_a}}{J_x \tau^2} \delta_a + \frac{\mu c_{L\delta_n}}{J_x \tau^2} \delta_n$$

$$(8 - 3) - \frac{\mu c_{n\beta}}{J_z \tau^2} \beta + \left(s - \frac{c_{n\dot{n}}}{2J_z \tau} \right) \dot{\psi} - \frac{c_{n\phi}}{2J_z \tau} \phi = \frac{\mu c_{n\delta_a}}{J_z \tau^2} \delta_a + \frac{\mu c_{n\delta_n}}{J_z \tau^2} \delta_n$$

$$\text{where } J_x = 2 \left(\frac{k_y}{b} \right)^2 \quad J_z = 2 \left(\frac{k_z}{b} \right)^2 \quad \mu = \frac{m}{\bar{\rho} S b} \quad \tau = \frac{m}{\bar{\rho} S U_0}$$

The parameters of airplane motion which were measured and available for feedback to the automatic pilot were sideslip angle, yaw rate, roll angle, roll rate, rudder pedal position and lateral stick position. Using these parameters, each with an associated feedback gain, the rudder and aileron control deflections were defined as:

$$(9 - 1) \delta_n = K_{14} \delta_R + K_4 \beta + K_5 \dot{\phi} + K_6 \dot{\psi} + K_7 \delta_A$$

$$(9 - 2) \delta_a = K_{13} \delta_A + K_8 \beta + K_9 \dot{\phi} + K_{10} \dot{\psi} + K_{11} \phi$$

The constants K_i are functions of the autopilot system and the range of values possible for these constants defines the limits of the possible simulation for any given configuration.

Combining Equations (9) and (7) yields the final set of equations for the artificial stability airplane:

$$(10 - 1) (s - \gamma_v'') \beta + (1 - \gamma_n'') \dot{\psi} - g/v_0 \phi = \gamma_n'' \delta_R$$

$$(10 - 2) - L''_{\beta} \beta - L''_n \dot{\psi} + (s^2 - L''_{p}s + L''_{\phi}) \phi = L''_{\delta_a} \delta_A + L''_{\delta_n} \delta_R$$

$$(10 - 3) - N''_{\beta} \beta + (s - N''_n) \dot{\psi} - (N''_{\dot{p}}s + N''_{\dot{q}}) \phi = N''_{\delta_a} \delta_A + N''_{\delta_n} \delta_R$$

The doubled primed "effective derivatives" are defined in terms of the K_1 in Table III. The derivatives N_ϕ'' and L_ϕ'' are artificial derivatives and are normally zero in real airplanes.

The equations for the equivalent stability derivatives as listed in Table III may be solved for the variable gain constants to yield a more usable form for simulating an aircraft of known stability derivatives in the following manner. Consider the following pair of equations:

$$\begin{aligned} L_\beta'' &= L_\beta + K_4 L_{\delta_n} + K_8 L_{\delta_a} \\ N_\beta'' &= N_\beta + K_4 N_{\delta_n} + K_8 N_{\delta_a} \end{aligned}$$

If the double primed derivatives are the desired values and the unprimed derivatives are the derivatives for the basic NAvion, the two equations may be written:

$$\begin{aligned} L_\beta'' - L_\beta &= K_4 L_{\delta_n} + K_8 L_{\delta_a} \\ N_\beta'' - N_\beta &= K_4 N_{\delta_n} + K_8 N_{\delta_a} \end{aligned}$$

Solving these two equations simultaneously for K_4 and K_8 gives:

$$\begin{aligned} K_4 &= \frac{(L_\beta'' - L_\beta) N_{\delta_a} - (N_\beta'' - N_\beta) L_{\delta_a}}{L_{\delta_n} N_{\delta_a} - N_{\delta_n} L_{\delta_a}} \\ K_8 &= \frac{(N_\beta'' - N_\beta) L_{\delta_n} - (L_\beta'' - L_\beta) N_{\delta_n}}{L_{\delta_n} N_{\delta_a} - N_{\delta_n} L_{\delta_a}} \end{aligned}$$

Numerical solutions for the various K_1 based on NAvion numerical derivatives are shown in Table IV.

In considering the over-all effect of varying the gain constants to satisfy a given set of stability derivatives it is necessary to examine the following equations:

$$Y_v'' = Y_v + K_4 Y_{\delta_n}$$

$$Y_n'' = K_6 Y_{\delta_n}$$

$$Y_p'' = K_5 Y_{\delta_n}$$

The derivative Y_v'' can be varied only at the expense of losing the independent variation of one of the more important derivatives L_{ϕ}'' or N_{ϕ}'' . In addition, the derivatives Y_r'' and Y_p'' which are normally considered negligible in conventional aircraft configurations are present for any non-zero values of K_5 and K_6 . However, due to the small magnitude of the basic NAVion derivative Y_{δ_r} these effects may be considered negligible for small values of the associated gain constants and it may be assumed that the only effect is that the derivative Y_v cannot be modified from the basic NAVion value. Also it should be noted that the term g/U_0 which corresponds to C_{L_0} can not be modified artificially with the present feedback scheme.

From the foregoing discussion it is concluded that a system such as the one proposed has the capability of varying all of the stability derivatives in Equation (10), except those appearing in the side-force equation. The range of variation is theoretically dependent only on the range of the K_1 available with the airplane-autopilot system. It is also noted that modifications to the numerator terms of the transfer function may be made as well as modification to the characteristic equation.

Numerical values for the basic NAVion stability derivatives were obtained from the "best average" of experimental and analytical determinations

as given by Refs. 6 and 7. The values used are tabulated in both dimensional and non-dimensional form in Table V. Dimensional derivatives are based on the following flight condition:

$$U_0 = 120 \text{ MPH}$$

$$h_p = 6,500 \text{ ft.}$$

$$W = 2800 \text{ lbs.}$$

SIMULATION OF AN ARBITRARY "X" AIRPLANE

In the selection of an arbitrary airplane to simulate, it was desired that the characteristics be appreciably different from those of the basic NAVion to indicate the simulation possibilities of the modified NAVion. In addition, it was desired that the characteristics lend themselves to the proposed investigation of the effect of variations in the $\frac{\omega_\phi}{\omega_d}$ ratio.

In a proposed lateral dynamic handling qualities test program, Cornell Aeronautical Laboratory has suggested response specifications for a hypothetical airplane which characterizes a "good equivalent airframe." This proposal is given in Ref. 8. Two values of the damping parameter ζ_d were suggested in order to cover both the satisfactory and unsatisfactory dutch roll damping ranges defined in current military handling qualities specifications. The smaller of the suggested values was chosen for this investigation. The suggested response specifications for the "X" airplane were:

$$T_R = 0.4 \text{ sec. } \frac{1}{T_S} < \frac{.08}{\text{sec.}} \quad \omega_d \doteq 2 \text{ rad/sec. } \zeta_d = .05$$

$$\frac{|\phi|}{|\beta|} \doteq 3 \quad L\zeta_a \left(\frac{\omega_\phi}{\omega_d} \right)^2 \sim \text{"good" region from pilot opinion}$$

Longitudinal characteristics "good" - satisfied by basic NAVion

The determination of numerical values for the desired stability derivatives to satisfy these conditions and determination of the necessary feedback gain constants are shown in Appendix A. The results of these calculations may be summarized as follows:

<u>Basic Airplane</u>	<u>"X" Airplane</u>
$Y_v = - 0.216$	
$g/U_0 = 0.183$	
$L_\beta = - 9.76$	$L_\beta'' = - 19.26$
$L_p = - 7.4$	$L_p'' = - 2.184$
$L_r = 1.95$	$L_r'' = 2.26$
$N_\beta = 4.81$	$N_\beta'' = 4.0$
$N_p = - 0.376$	$N_p'' = 0.122$
$N_r = - 0.416$	$N_r'' = - 0.30$

K_i	Numerical Value	$\frac{\omega_d}{\omega_d}$	$\frac{N\delta a''}{L\delta a''}$	δ_x
K_4	0.248	0.5	- 0.156	0.915
K_5	- 0.152	0.8	- 0.075	0.393
K_6	- 0.046	1.0	0	- 0.0492
K_8	- 0.484	1.2	0.092	- 0.542
K_9	0.271			
K_{10}	0.020			
K_{11}	0			

It was not found necessary to utilize the artificial derivatives N_{ϕ}'' and L_{ϕ}'' in the simulation.

The major modifications to the basic NAVion were seen to be:

- (1) a large increase in positive dihedral effect,
- (2) a large decrease in the damping in roll,
- (3) a moderate decrease in the damping in yaw, and
- (4) a change of sign of the yaw due to roll derivative.

The change in sign of the yaw due to roll which was required to satisfy the specifications of the "X" airplane, although unorthodox, could occur for airframe configurations with low aspect ratio wings and a large vertical fin which is characteristic of many high performance aircraft. For example, flight test results for the F-100 cited in Ref. 9 show a positive value for the derivative in certain high speed flight conditions.

Due to the validity condition for the dutch roll damping approximation, shown in Appendix A, some doubt existed as to the achievement of a S_d value of 0.05. The lack of simple and accurate approximations for dutch roll damping makes this aspect of simulation predictions difficult.

Variation of the parameter $\frac{\omega_\phi}{\omega_d}$ over the range 0.5 to 1.2 was selected in order to study the extremes of the ranges suggested in Ref. 2 and 8. In particular it was considered desirable to determine whether $\frac{\omega_\phi}{\omega_d} = 0.5$ would produce roll rate reversal as predicted in Ref. 2.

The computed values for the feedback gain constants were within the capability of the modified NAVion, the signs of the numerical values dictating the polarity of the variable feedback loops. The required values of K_6 and K_{10} , however, were impossible to obtain to any predictable accuracy without extensive circuitry changes in the autopilot system. The effect of the parameters associated with K_6 and K_{10} on the motions of the simulated aircraft is discussed in the analysis of analog computer results.

The necessary gain potentiometer settings required in the NAVion to achieve the desired values of the K_1 and δ_x are shown in the calibration curves of Figs. 12 through 19.

ANALOG COMPUTER STUDY

An analog computer study was made using an electrical analog of the variable-stability NAVion and the calculated values of the feedback gains necessary to simulate the "X" airplane.

The purpose was:

- (1) To ascertain the degree of simulation possible from the approximate calculation methods used;
- (2) To determine the range of the aircraft control deflections necessary to accomplish the simulation in order to determine the limitations of the modified NAVion in simulating the "X" airplane;

- (3) To study the effect of varying the ratio $\frac{\omega\phi}{\omega_d}$ on the time response with predictions which may be made from Equation (4).

Using the equations of motion expressed in dimensional derivatives and real time, Equations (7), the required computer circuitry was designed so that the potentiometer settings represented the derivatives, thus facilitating the association of the equations with the computer circuitry. Separate summing networks were designed to produce rudder and aileron control deflection proportional to the appropriate airplane motions so that the stability derivatives could be modified on the computer in the same manner as in the modified NAVION. Computer circuit diagrams are shown in Fig. 21 and Fig. 22. The computer equations and potentiometer settings are given in Table V.

The forcing functions used to study the characteristics of the motion of the "X" airplane were a step aileron input to obtain the rolling velocity response and a combined rudder and aileron pulse to excite the dutch roll mode of motion. A two degree step was chosen in order to provide a uniform input for the entire range of variation of the $\frac{\omega\phi}{\omega_d}$ ratio. This magnitude of the step function was low enough to allow sufficient time for a steady state roll rate to be reached before attaining an excessive roll angle and yet large enough to provide a measurable response.

The time-traces from the computer runs are shown in Fig. 23 through Fig. 27. The results of measurement of the parameters of interest, made from these time-traces, are given in Table VII.

Some difficulty in obtaining consistent measurements from the time-traces was experienced. In particular, the dutch roll damping ratio, the magnitude of the first overshoot of the roll rate and the magnitude of the steady state rolling velocity were difficult to measure accurately. In analysis of the time-traces, the influence of the spiral mode was assumed negligible for the first three seconds. The damping ratio was determined by constructing the envelopes of the dutch roll traces, measuring the magnitudes from the mean line to two successive peaks and converting the ratio of the amplitudes to damping ratio by use of charts given in Ref. 10. The accuracy in measuring the correlation parameter for $\frac{\omega_\phi}{\omega_d}$ ratios near unity is doubtful, due primarily to the relatively low rolling velocities attained.

The results of the time-trace analysis showed good simulation of the response specifications of the "X" airplane with the exception that dutch roll damping was higher than desired. This possibility had been anticipated, and was discussed previously. It was found analytically and verified by the computer study that the magnitudes of the yaw-rate feedbacks required for the modification of the derivatives N_r and L_r were very small. Due to the improbability of any appreciable accuracy in attaining the potentiometer settings required to supply these small feedbacks in the modified NAVion, it was decided to leave these derivatives unmodified. This condition could be alleviated through a modification of circuitry by using dropping resistors or by reducing the excitation voltage on the yaw rate transducers. Changing the summing circuitry by the use of dropping resistors to improve potentiometer resolution had been tried in the pitch channel, resulting in quadrature and threshold problems arising within

the amplifier-calibrator unit. For this reason, no such modification was attempted in the roll or yaw channels. The result of leaving these derivatives unmodified was seen from the analog traces to be an increase in the dutch roll damping and a change from a slightly divergent to a slightly convergent spiral mode. These effects are readily predicted by referring to the approximations for the spiral and dutch roll damping terms of the characteristic equation. The necessity for further investigation to determine compatible relations between the ratio adjustments and the feedback gains used in the autopilot circuitry is indicated.

The range of control deflections necessary for the simulation were seen from the analog study to be well within the range available in the NAVion.

The results of the analog study clearly showed that departure of the ratio $\frac{\omega_{\phi}}{\omega_d}$ from unity was reflected by an increased magnitude of the induced dutch roll oscillation in response to an aileron step input. In addition, a rolling rate reversal had already occurred for $\frac{\omega_{\phi}}{\omega_d} = 0.5$. An increase in the value of the $\frac{\omega_{\phi}}{\omega_d}$ ratio produced an increase in the steady state roll rate attained for the same input magnitude. All of these effects, except the premature rolling reversal are predictable from Equation (4).

The computer study showed no major theoretical limitations to the use of the modified NAVion as a lateral-directional flight simulator. The problem of obtaining a large fractional change in a small derivative, such as N_r , has been discussed, and this problem would apply to other small derivatives. The only other limitations which could be anticipated from

the computer study were those associated with the airplane instrumentation. The magnitudes of the physical quantities sensed in the feedback loops were approaching the mechanical limits of the transducers used in the autopilot.

FLIGHT PHASE

The experimental phase of the investigation consisted of a limited flight test program. The primary purpose of the flight test program was to obtain a preliminary evaluation of the modified NAVion as a lateral-directional flight simulator. Accuracy and repeatability of simulation conditions are vital prerequisites for subsequent utilization of the NAVion in any meaningful study of handling qualities parameters. As a secondary objective, an attempt was made to obtain some indication as to the feasibility of the proposed pilot opinion study of the parameter $\frac{\omega_{\phi}}{\omega_d}$. It must be noted, however, that the flight maneuvers used were designed to reflect the degree of simulation and were not necessarily those which might best reflect pilot opinion. No quantitative rating of pilot opinion was attempted. For these reasons, all pilot opinion expressed in the subsequent discussion must be interpreted as "first impression."

From the combined results of the various phases of the investigation preliminary to the flight test phase, several qualitative observations were made:

- (1) With the exception of minor threshold and resolution difficulties discussed previously, the modified NAVion should be capable of a wide range of controlled dynamic simulation in the lateral-directional modes of motion.

- (2) Due to the fact that the NAVion is a low-speed, low-altitude airplane not designed for high maneuverability or acrobatic flight, some difficulty was anticipated in meeting some of the current military specifications for fighter type aircraft.
- (3) The speed limitations of the NAVion makes it impossible to simulate the accelerations experienced in any similar maneuver in a high speed aircraft. This would probably have a measurable effect on pilot opinion ratings.

From the first few evaluation flights of the modified NAVion, several deficiencies were noted in the system:

- (1) Resolution in trimming the aircraft by use of the knob- actuated trim controller was not adequate for the precision trim adjustments necessary in the flight test maneuvers. This could be alleviated by adjusting the "peck size" of the autopilot system, or by increasing the mechanical gear ratio of servo-drum travel to aileron control surface deflection.
- (2) The combination of low gain potentiometer settings required and the resolution obtainable from the markings on the potentiometer face-plates adversely affected the repeatability of precise feedback gain settings. The problem of the low feedback settings has been discussed. Installation of vernier type potentiometers would improve the repeatability of settings.
- (3) Changing the polarity of the lateral stick deflection to rudder channel signal required removal of the main terminal board from the equipment table. Relocation of the necessary terminals to a more accessible part of the terminal board is indicated.

(4) Large amounts of cable stretch in the aircraft control systems, particularly the aileron system, due to airloads on the control surfaces invalidated the control deflection calibration made on the ground. This problem is one of great importance since it affects the variation of all the equivalent stability derivatives. This problem might possibly be solved by installing control surface position transducers at each aileron and at the rudder. This would permit an airborne calibration of control surface position per volt input to the autopilot. This problem had also be noted in Ref. 6.

The flight test maneuvers were patterned after the forcing function inputs used on the analog computer. These were a step aileron input to obtain roll rate response and a cross-controlled maneuver to excite the dutch roll oscillation. It was found, during the preliminary flights, that a satisfactory entry for the rolling maneuver was to trim the airplane initially to a steady side-slip condition. This entry allowed sufficient time for the airplane to reach a satisfactory steady state roll rate before too large a bank angle had developed with an associated tendency for the airplane to enter a steep nose-down spiral. The special auxiliary circuit providing the step aileron input, described in Section II, was adjusted on the ground to provide a static aileron deflection of 10° . This constant input was used in all rolling maneuvers. Due to the cable stretch in the aileron control system, the actual deflection of the ailerons in flight was less than 10° . It was estimated to be approximately 3 - 4 degrees. The dutch roll entry was effected by establishing a steady

side-slip condition by cross controlling the rudder and aileron flight controls and then rapidly releasing them.

The response of the airplane during the maneuvers was monitored through the telemetering ground station and the quality of the data was evaluated. This procedure permitted repeats of unsatisfactory maneuvers and facilitated the flight test program by enabling good quality data to be obtained in the limited flight time available.

Flight test runs consisted of a dutch roll excitation and the standard roll maneuver for each of six different configurations. The configurations consisted of the basic NAVion, the "X" airplane with no modification of the $\frac{\omega\phi}{\omega_d}$ ratio and the "X" airplane with the $\frac{\omega\phi}{\omega_d}$ ratio modified to values of 0.5, 0.8, 1.0, and 1.2.

The filtered time traces of telemetered time-histories of the flight maneuvers are shown in Figs. 23 through 27. The δ_a data was obtained from the servo-position data and the static ground calibration of aileron position angle. Measurements made from these traces and the analog computer traces are tabulated in Table VII.

For the basic NAVion, comparison of the results of analog and flight test data indicated excellent correlation in dutch roll period and damping and fair correlation in the measured $\frac{|\phi|}{|\beta|}$ and $\frac{|P_1|}{P_{3s}}$ ratios. A comparison of steady state rolling velocity would be meaningless due to the uncertainty in measuring the aileron position angle and the rolling root $1/T_R$ from the flight test results.

The dutch roll frequency of the "X" airplane shows excellent correlation with analog results. The value of the dutch roll damping parameter however, was seen to be about 0.20 from flight test data as opposed to

0.10 from analog results. The flight test value for the $\frac{|\dot{\phi}|}{|\beta|}$ ratio was about 0.9 as opposed to 3.0 from the analog results. A change in the dihedral effect smaller than that predicted would tend to induce errors in both of these parameters in the direction indicated by the comparison of results. At least a part of these apparent discrepancies may be attributed to the aileron system cable stretch. Whether the dynamic characteristics of the autopilot or sensing devices contributed significantly to these differences is not known. Some non-linear effects were noted in the flight test data from the "X" airplane configuration, but these effects were small and the causes were not investigated.

Difficulties in repeatability of gain potentiometer settings are indicated by the differences in dutch roll damping of the flight maneuvers for $\frac{\omega_{\phi}}{\omega_d} < 1$ and those for $\frac{\omega_{\phi}}{\omega_d} > 1$. These sets of data were obtained from two separate flights, which required re-setting all of the gain potentiometers.

Although over-all simulation was not considered good from comparison of flight test and analog results, it is apparent from the results that the variable feedback autopilot system has the capability of considerable variation of the characteristics of the NAVion. It is believed that with the modifications to the system which have been proposed, the modified NAVion would be capable of acceptable simulation over a considerable range of characteristic motions.

From the flight test data obtained for the various predicted values of the $\frac{\omega_{\phi}}{\omega_d}$ ratio, the qualitative effect on the variation of the induced dutch roll oscillations was the same as that shown by the analog computer traces. The amplitude of dutch roll oscillations increased with departure

of the $\frac{\omega_\phi}{\omega_d}$ ratio from unity and the steady state roll rate increased with increasing $\frac{\omega_\phi}{\omega_d}$. There was little correlation in the magnitude of these effects, however. Roll rate reversal had already occurred at a predicted value of the $\frac{\omega_\phi}{\omega_d}$ ratio of 0.8 in the flight test data while the analog results showed the upper limit of this phenomenon to be at $\frac{\omega_\phi}{\omega_d} = 0.6$.

From the $\frac{\omega_\phi}{\omega_d}$ ratio;

$$\left(\frac{\omega_\phi}{\omega_d}\right)^2 \doteq 1 - \frac{N\delta_c'' L\beta''}{L\delta_c'' N\beta''}$$

it can be seen that discrepancies in the simulation of either the control derivatives, $L\beta''$, or $N\beta''$ could cause variance in the actual value attained. Cable stretch in both the aileron and rudder control systems, affecting all of these derivatives, may induce significant errors in this ratio. The flight test run for a predicted $\frac{\omega_\phi}{\omega_d}$ ratio of 0.5 showed not only roll rate reversal, but also a turn in the wrong direction for the step input. This was not predicted in the computer study.

Calculation of the $\frac{\omega_\phi}{\omega_d}$ ratio from the correlation parameter equation depends on the ability to measure $1/T_R$. Since the input for the rolling maneuver was approximately a ramp-type input rather than a step, data reduction procedures similar to those outlined in Ref. 11 are indicated. It would be desirable to have available a rapid means to check the accuracy of the equivalent stability derivatives. Perhaps, some sort of analog matching technique could be employed.

The basic stick-steering autopilot was satisfactory. The control deflections required to fly the basic NAVION were easily obtained by adjusting the flight control gain potentiometers to a desired setting. It was suggested by the pilots who flew the airplane that the rudder pedal spring tension be increased, and that the stick flight controller damping be decreased.

The motion of the modified NAVion in the test configurations was very pronounced. It was quite apparent to the pilots that, because of the very effective airplane control surfaces, the basic modes of motion of the basic airplane had been substantially changed. In particular, the dutch roll mode of motion was easily excited for the "X" airplane, and in some cases very difficult to control. For the low speeds and the low roll rates used in this investigation, the pilots were not able to distinguish small changes in the correlation parameter $\frac{|P_1|}{P_{ss}}$. For high speeds and high roll rates, small changes might well be noticeable both from the magnitude of the roll rate oscillation and the induced accelerations. This indicates that any numerical "satisfactory limits" placed on either the $\frac{\omega_d}{\omega_n}$ ratio or the correlation parameter would probably have to be a function of the anticipated roll rates in order to be of value as flying quality criteria.

The utility of using the NAVion class airplane to obtain valid pilot-opinion data appears to be limited perhaps just to indicate a trend or range of pilot opinion. The airplane does provide, however, a six degree of freedom platform at relatively low cost, and should be useful in developing techniques utilized in a more general study.

SECTION IV

CONCLUSIONS

The preliminary evaluation of the North American NAVion class airplane as a lateral-directional variable stability flight simulator for use in the investigation of handling qualities criteria resulted in the following conclusions:

1. The NAVion, configured with a three-axis variable feedback autopilot, is capable of simulation over a considerable range of the lateral-directional modes of motion.
2. The use of the NAVion as a flight simulator to obtain accurate quantitative pilot-opinion data which are valid for high speed, highly maneuverable aircraft appears to be limited, due to the flying qualities of the basic airplane. The convenience and the relatively modest cost of the NAVion as a six degree of freedom simulator, however, indicate its value for limited range studies of pilot-opinion trends.
3. The ratio $\frac{\omega_q}{\omega_d}$ and its correlation parameter, $\frac{|R|}{R_s}$, are perhaps valid handling qualities criteria, but any numerical limits assigned should be functions of the anticipated rolling velocities.

TABLE I

PHYSICAL CHARACTERISTICS OF THE NAVION

WING DATA

Total Area (including ailerons, flaps and 19.87 ft. covered by fuselage)	184.34 ft. ²
Span	33.38 ft.
Aspect Ratio	6.05
Taper Ratio	0.54
Dihedral Angle	7.50 deg.
Root Chord	7.20 ft.
Mean Aerodynamic Chord	62.35 in.
Incidence Angle	
Root	2.0 deg.
Tip	- 1.0 deg.
Sweepback of Leading Edge	3.0 deg.
Twist	
Geometric	3.0 deg.
Airfoil Section	
Root	NACA 4415R
Tip	NACA 6410R
Flaps, 40 deg., Plain	

AILERON DATA (For one aileron)

Area	2.16 ft. ²
Span	61.99 in.
Deflection	30 deg. up; 20 deg. dwn.

TABLE I (continued)

AILERON DATA (continued)

Control	Wheel Throw
Aerodynamic Balance	Frise-type nose
Static Balance (Outboard end of each aileron)	Streamlined weight
Trim Tab (Right aileron)	Fixed Bend Tab
Ratio of Aileron Chord to Wing Chord	0.284

HORIZONTAL TAIL DATA

Total Area (Including 2.37 ft. ² covered by fuselage)	43.05 ft. ²
Span	13.17 ft.
Aspect Ratio	4.02
MAC	3.34 ft.
Airfoil Sections, Root and Tip	NACA 0012
Incidence Angle	- 3.0 deg.

ELEVATOR DATA

Total Area	14.10 ft. ²
Span	73.58 in.
Deflection	30 deg. up; 20 deg. dwn.
Deflection Trim Tabs (32 in. span, 4-1/2 in. Chord)	\pm 30 deg.
Root Chord	1.5 ft.
Tip Chord	1.0 ft.

TABLE I (continued)

VERTICAL TAIL DATA

Area (Including 2.57 ft. ² blanketed by fuselage and excluding 1.84 ft. ² dorsal fin area)	12.93 ft. ²
Span	4.05 ft.
Airfoil Section	
Root	NACA 0013.2 Modified
Tip	NACA 0012-64 Modified
Incidence Angle (With respect to FRL)	2 deg. Nose Left

RUDDER DATA

Area	6.05 ft. ²
Deflection	17 deg. L.; 23 deg. R.
Trim Tab	Fixed Bend Tab
Rig (Angle with respect to fin center line)	3 deg. Right

FUSELAGE DATA

Fuselage Length Over-all	27.25 ft.
Width, Maximum	4.14 ft.
Depth, Maximum	4.40 ft.
Fineness Ratio	6.2

POWER PLANT DATA

Airplane is powered by one Continental E-185 engine. Maximum continuous rated horsepower at sea level 185 at 2300 RPM.

TABLE I (continued)

POWER PLANT DATA (continued)

The propeller is a Hartzell hydro-selective propeller with the following characteristics:

Activity Factor	100
Diameter	86 in.
Pitch (.75R)	26.5 deg.

MISCELLANEOUS DATA

Weight

Basic	2129 lbs.
Fuel (40 gal.)	240 lbs.
Pilots (2 with parachutes)	<u>410</u> lbs.
Gross Weight	2779 lbs.
Center of Gravity Position	29.5% MAC
Tail Length	16.88 ft.

Autopilot Mechanical Gear Ratios

Deg. Elevator per Deg. Servo-drum	0.919
Deg. Aileron per Deg. Servo-drum	0.910
Deg. Rudder per Deg. Servo-drum	0.330

TABLE II

SPECIFICATIONS OF INSTRUMENTATION COMPONENTS

RATE GYROS

Manufacturer	Minneapolis-Honeywell
Model No.	JG 7005A-24
Power Input	115 volts, 400 cycle A.C.
Power Consumption	32 watts (starting), 13 watts (running)
Rotor Speed	20,000 RPM
Weight	1.75 lbs.
Maximum Turn Rate	Modified to approximately 30° /sec.
Potentiometer Resistance	530 ohms
Potentiometer Excitation	Gyro #9 - 24 volts A.C. Gyros #10, #11 and #13 - 30 volts A.C.

VERTICAL GYRO (ROLL-PITCH)

Manufacturer	Minneapolis-Honeywell
Model No.	JG 7003A-11
Power Input	115 volts, 400 cycle A.C. 30 watts (max.)
Rotor Speed	20,000 RPM
Weight	4.5 lbs.
Potentiometer Active Angle	52° either side of center
Potentiometer Excitation	30 volts A.C.

TABLE II (continued)

SIDESLIP VANE

Manufacturer	Giannini
Model No.	2516
Potentiometer Resistance	1997 ohms
Potentiometer Active Angle	Yaw channel - $\pm 30^{\circ}$ Roll Channel - $\pm 45^{\circ}$
Potentiometer Excitation	Yaw channel - 15 volts A.C. Roll channel - 30 volts A.C.

TELEMETER TRANSMITTER UNIT

Manufacturer	ASCOP
Model No.	DT-4
Input Signals	0-5 volts D.C.
Information Channels	43 plus two for synchronization of ground station
Sampling Rate	20 RPS
Accuracy	$\pm 1\%$ of full scale
RF Power Output	4 watts
Frequency Range	215-235 MC
Frequency Stability	$\pm 0.05\%$
Primary Power Requirement	28 volts D.C.
Weight	19.6 lbs.

TABLE II (continued)

MISCELLANEOUS DATA

Excitation Voltages

Servo Position Potentiometers	Roll Channel	48 volts A.C.
	Yaw Channel	60 volts A.C.
Trim Controller		30 volts A.C.
Rudder Pedal Position		40 volts A.C.
Stick Controller (Roll)		35 volts A.C.
Feedback Gain Potentiometer		5000 ohms
Resistance		

TABLE III
DEFINING EQUATIONS FOR EQUIVALENT
AND
ARTIFICIAL STABILITY DERIVATIVES

$$L_{\delta}'' = L_{\delta} + K_4 L_{\delta r} + K_8 L_{\delta a}$$

$$N_{\delta a}'' = K_{13} N_{\delta a} + K_7 N_{\delta r}$$

$$L_r'' = L_r + K_6 L_{\delta r} + K_{10} L_{\delta a}$$

$$N_{\delta r}'' = K_{14} N_{\delta r}$$

$$L_p'' = L_p + K_5 L_{\delta r} + K_9 L_{\delta a}$$

$$Y_v'' = Y_v + K_4 Y_{\delta r}$$

$$L_{\delta a}'' = K_{13} L_{\delta a} + K_7 L_{\delta r}$$

$$Y_r'' = K_6 Y_{\delta r}$$

$$L_{\delta r}'' = K_{14} L_{\delta r}$$

$$Y_p'' = K_5 Y_{\delta r}$$

$$N_{\delta}'' = N_{\delta} + K_4 N_{\delta r} + K_8 N_{\delta a}$$

$$Y_{\delta r}'' = K_{14} Y_{\delta r}$$

$$N_r'' = N_r + K_6 N_{\delta r} + K_{10} N_{\delta a}$$

$$L_{\phi}'' = K_{11} L_{\delta a}$$

$$N_p'' = N_p + K_5 N_{\delta r} + K_9 N_{\delta a}$$

$$N_{\phi}'' = K_{11} N_{\delta a}$$

TABLE IV

NUMERICAL SOLUTIONS FOR FEEDBACK GAIN CONSTANTS

$$K_4 = 1.312 - .002415 L_{\beta}'' - .2775 N_{\beta}''$$

$$K_5 = - .123 - .002415 L_p'' - .2775 N_p''$$

$$K_6 = - .124 - .002415 L_r'' - .2775 N_r''$$

$$K_8 = .346 + .0490 L_{\beta}'' + .0278 N_{\beta}''$$

$$K_9 = .373 + .0490 L_p'' + .0278 N_p''$$

$$K_{10} = - .0828 + .0490 L_r'' + .0278 N_r''$$

$$\frac{K_7}{K_{13}} = - \left[\frac{20.5 \frac{N_{\delta_a}''}{L_{\delta_a}''} + .178}{2.05 \frac{N_{\delta_a}''}{L_{\delta_a}''} + 3.62} \right] = \delta_x$$

TABLE V

NUMERICAL VALUES FOR BASIC NAVION STABILITY DERIVATIVES

The values of the non-dimensional derivatives given are values averaged from several methods of stability derivative determination as given in previous NAVion lateral-directional studies and summarized in Ref. 7.

<u>Non-dimensional Derivative</u>	<u>Value</u>	<u>Dimensional Derivative</u>	<u>Value</u>
$C_{y\beta}$	-.592	Y_v	-.216
C_{l_r}	.117	L_r	1.95
$C_{l\beta}$	-.0554	L_β	-9.76
C_{l_p}	-.441	L_p	-7.4
C_{n_r}	-.0932	N_r	-.461
$C_{n\delta_a}$	-.0034	N_{δ_a}	-.178
$C_{n\beta}$.0918	N_β	4.81
C_{n_p}	-.0758	N_p	-.376
$C_{y\delta_r}$.158	Y_{δ_r}	.0576
$C_{l\delta_a}$.115	L_{δ_a}	20.5
$C_{l\delta_r}$.0116	L_{δ_r}	2.05
$C_{n\delta_r}$	-.0691	N_{δ_r}	-3.62

Transformation from non-dimensional to dimensional form was based on the following conditions:

$$h = 6500 \text{ feet SDA}$$

$$U_o = 120 \text{ MPH}$$

$$\tau = 1.37 \text{ sec.}$$

$$\mu = 7.24$$

$$J_x = .0218$$

$$J_z = .0735$$

TABLE VI
ANALOG EQUATIONS
AND
POTENTIOMETER SETTINGS

Potentiometer numbers and analog circuitry are shown in Figs. 21 and 22.

EQUATIONS

$$\begin{aligned} -\ddot{\beta} &= .216 \beta + \dot{\psi} - .1825\dot{\phi} - .0576 \delta_r \\ -\ddot{\phi} &= 9.76 \beta - 1.95 \dot{\psi} + 7.4\dot{\phi} - 20.5 \delta_a - 2.05 \delta_r \\ -\ddot{\psi} &= -4.81\beta + .461 \dot{\psi} + .376 \dot{\phi} + .178 \delta_a + 3.63 \delta_r \\ \delta_r &= \pm P_7 \delta_A + P_4 \beta - 0.1 P_6 \dot{\psi} - P_5 \dot{\phi} \\ \delta_a &= P_{13} \delta_A - P_8 \beta + 0.1 P_{10} \dot{\psi} + 0.5 \times P_{11} \dot{\phi} + P_9 \dot{\phi} \end{aligned}$$

POTENTIOMETER SETTINGS

Pot#	Represents	Setting	Pot#	Represents	Setting
1	Y_v	.216	13	K_{13}	Variable
2	$2 g/U_o$.365	15	.1 L_p	.74
3	$5 Y\delta_r$.288	16	.05 L_β	.488
4	K_4	.248	17	.25 $L\delta_r$.5125
5	$-K_5$.152	18	.25 L_r	.4875
6	$-10K_6$	0	19	.025 $L\delta_a$.5125
7	$\pm K_7$	Variable	20	$2 N\delta_a$.356
8	$-K_8$.484	28	N_p	.376
9	K_9	.271	29	N_r	.461
10	$10 K_{10}$	0	30	.2 $N\delta_r$.725
11	$2 \frac{K_{11}}{X}$	0	31	.1 N_β	.481

TABLE VII

COMPARISON OF FLIGHT TEST AND ANALOG DATA

CON- FIGURATION	BASIC NAVION $\frac{\omega_d}{\omega_d} = .92$		"X" $\frac{\omega_d}{\omega_d} = 0.5$		"X" $\frac{\omega_d}{\omega_d} = 0.8$		"X" $\frac{\omega_d}{\omega_d} = .96$		"X" $\frac{\omega_d}{\omega_d} = 1.0$		"X" $\frac{\omega_d}{\omega_d} = 1.2$	
	COMP	TEST										
Parameter			COMP	TEST	COMP	TEST	COMP	TEST	COMP	TEST	COMP	TEST
P_{av} (sec)	2.72	2.60	3.10	3.40	3.10	3.20	3.10	3.25	3.10	3.30	3.10	3.20
$T_{1/2}$ (sec)	2.17	2.10	3.40	1.80	3.40	1.85	3.40	1.75	3.40	2.00	3.40	2.00
$C_{1/2}$.799	.806	1.09	0.53	1.09	0.58	1.09	0.54	1.09	0.61	1.09	0.63
J_d	.138	.137	.100	.205	.100	.190	.100	.200	.100	.175	.100	.175
ω_d ($\frac{\text{rad}}{\text{sec}}$)	2.31	2.42	2.03	1.85	2.03	1.96	2.03	1.94	2.03	1.92	2.03	1.97
$\dot{\phi}_{ss}$ (0/sec)	4.60	8.60	4.0	- 5	10.1	1	15.0	11.0	15.6	11.5	21.5	17.0
$\left \frac{p_1}{p_{ss}} \right \%$	9.8	12.8	160	?	17.9	725	6.65	4.35	6.4	8.69	15.1	?
$\left \frac{\phi}{\beta} \right $.60	.416	3.08	.95	3.08	.75	3.08	.84	3.08	1.0	3.08	1.0

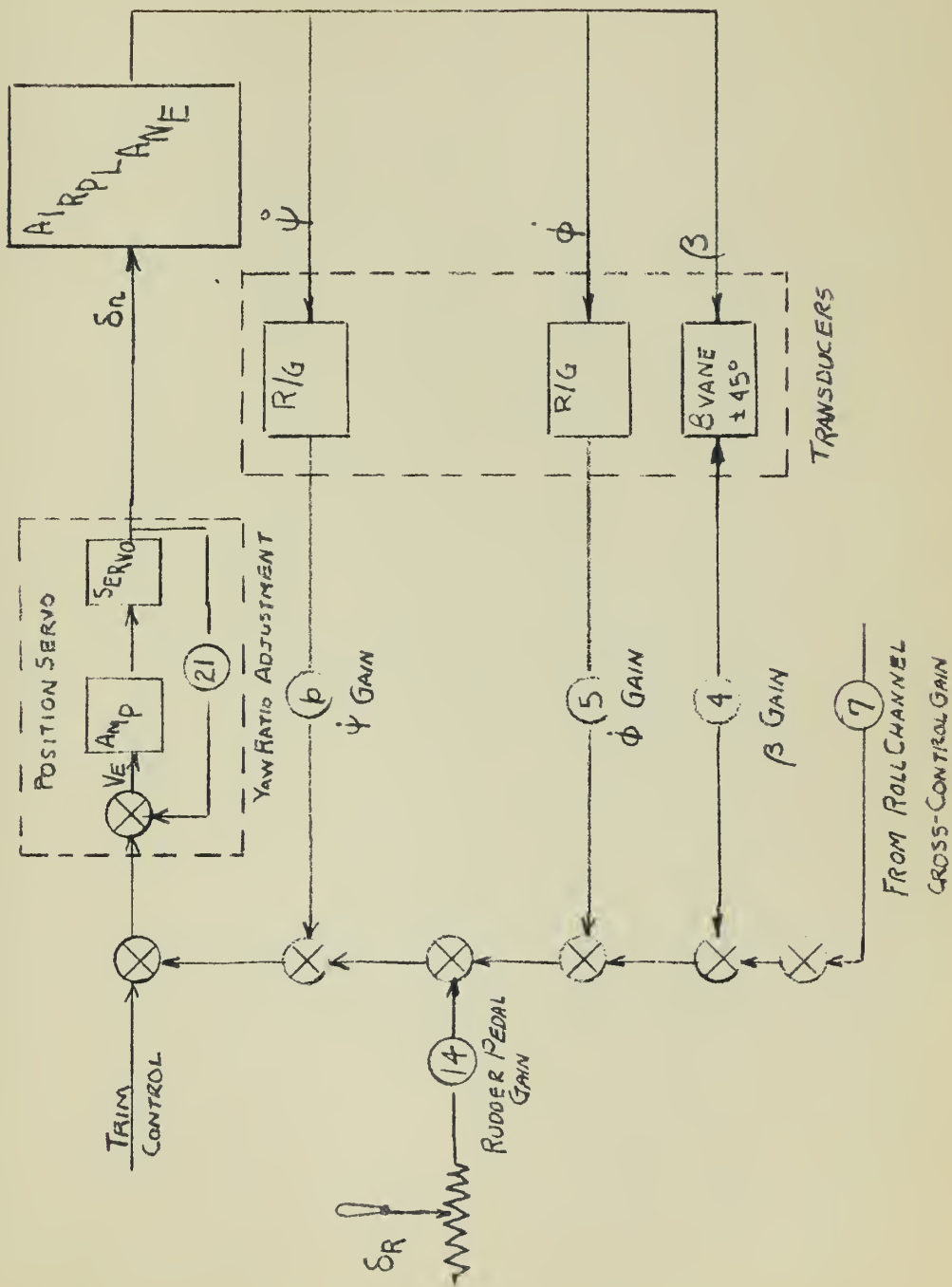
Notes: (1) Analog computer

(2) Flight test

FIGURE 1
TEST AIRPLANE



1. AIRSPEED BOOM
2. VANE BOOM



YAW CHANNEL

FIG 2
AUTOPILOT BLOCK DIAGRAM
NAVION

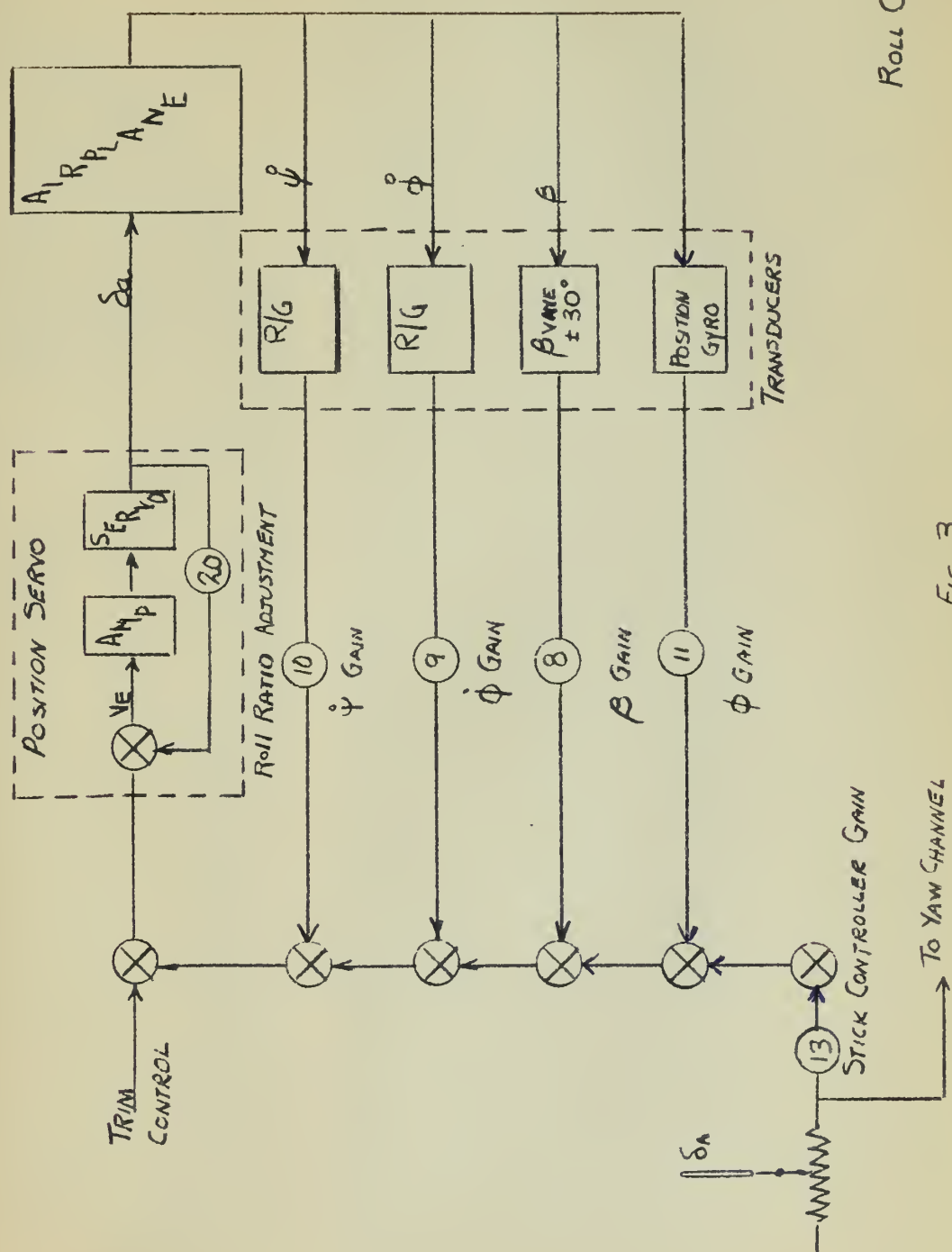


FIG. 3
AUTOPILOT BLOCK DIAGRAM
NAVION



FIGURE 4

GAIN POTENTIOMETER PANEL

FIGURE 5
EQUIPMENT COMPARTMENT
(TOP VIEW)

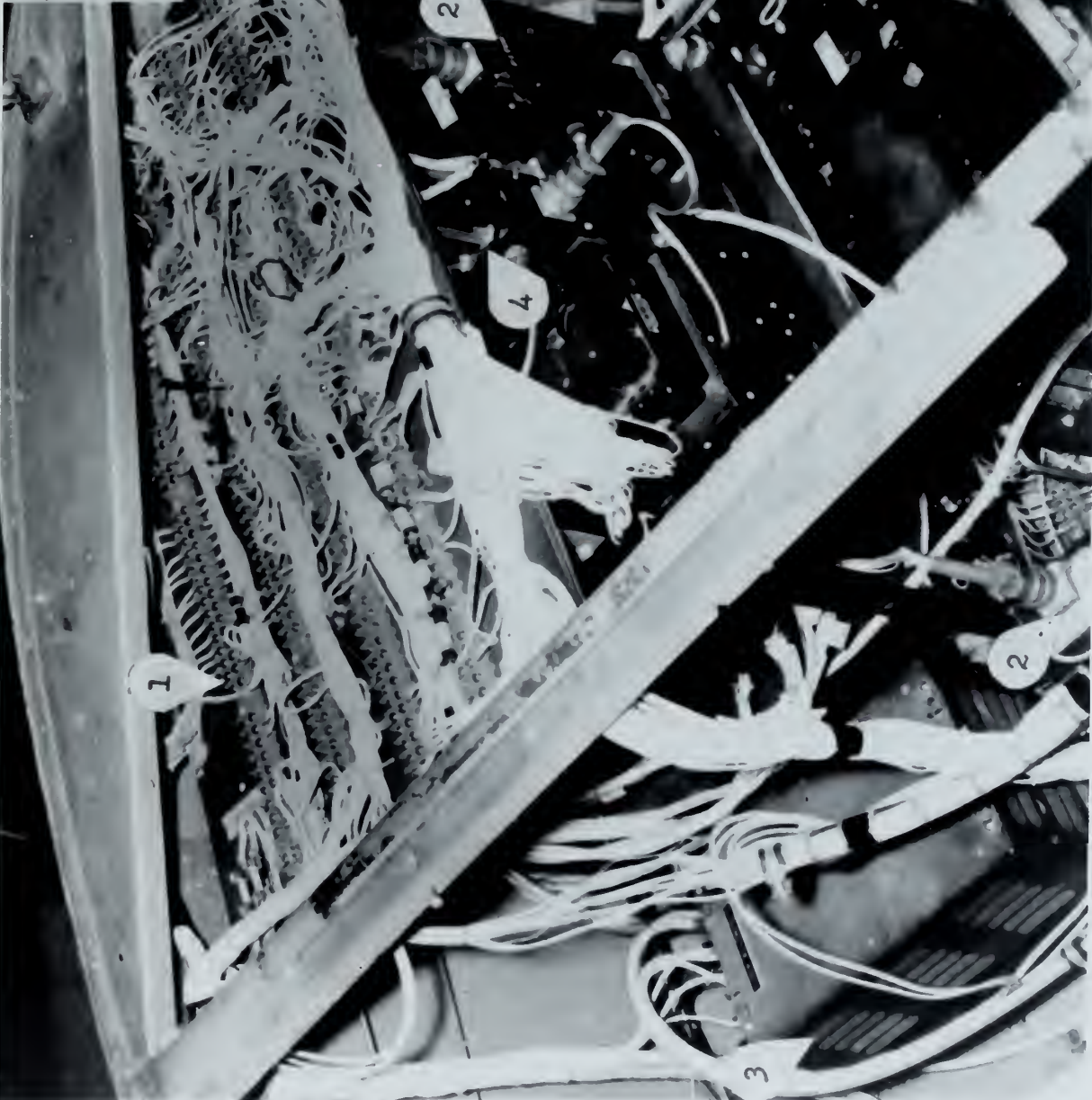
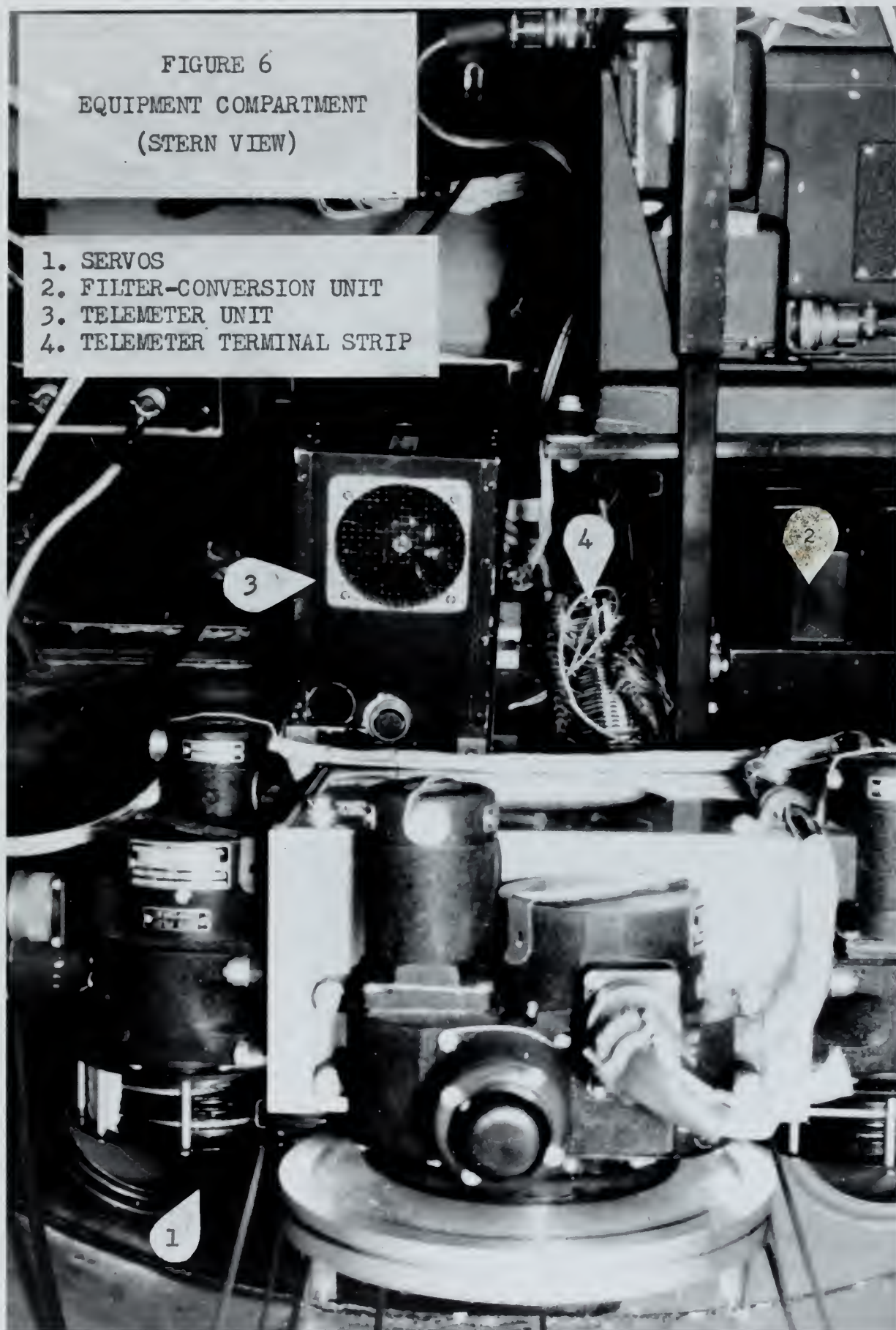
- 
- The photograph shows a top-down view of a complex equipment compartment. A large, dense bundle of white cables is on the left, labeled '1'. A long, thin metal beam runs diagonally across the center. To the right of the beam, there are several electronic components and more wiring, labeled '2', '3', and '4'. The background is dark and filled with various mechanical parts and structural elements.
- 1. MAIN TERMINAL BOARD
 - 2. RATE GYROS
 - 3. INVERTER
 - 4. ELECTRONIC CUT-OUT

FIGURE 6
EQUIPMENT COMPARTMENT
(STERN VIEW)

1. SERVOS
2. FILTER-CONVERSION UNIT
3. TELEMETER UNIT
4. TELEMETER TERMINAL STRIP



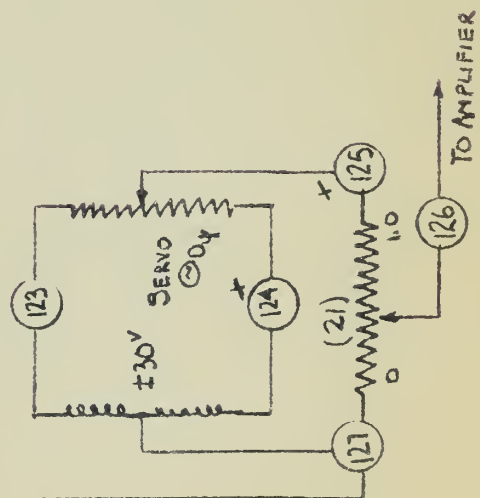
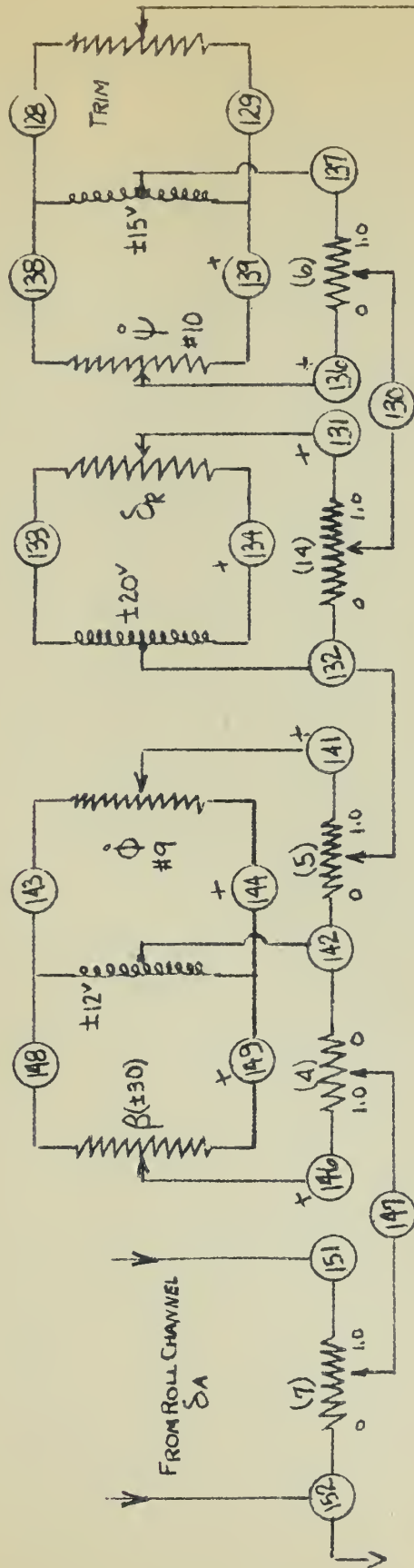
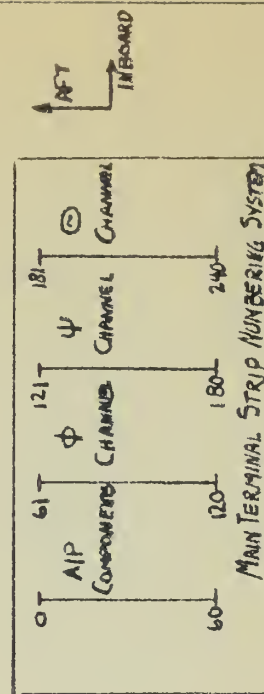
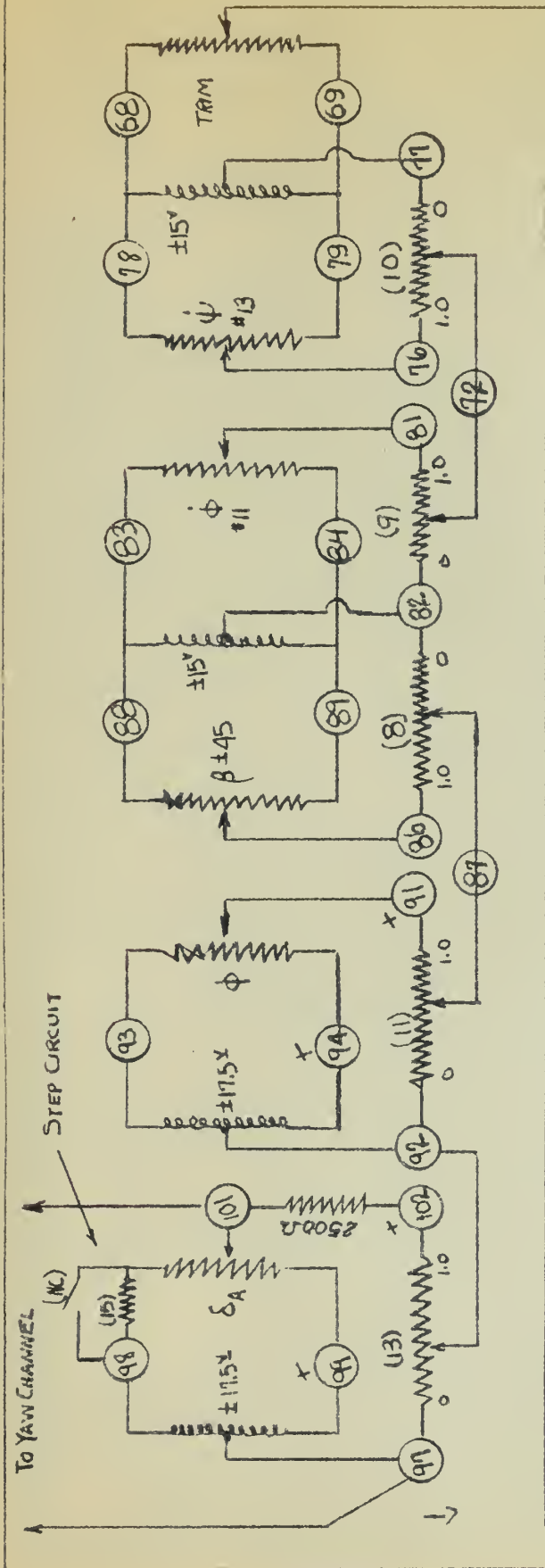


FIG. 7
AUTOPILOT SUMMING CIRCUIT
NAVION

NOTE: OTHER SYMBOLS FIG 8



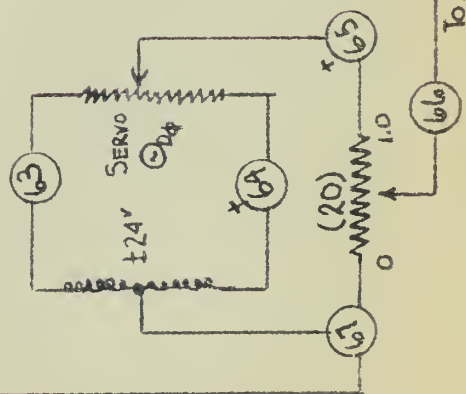
YAW CHANNEL



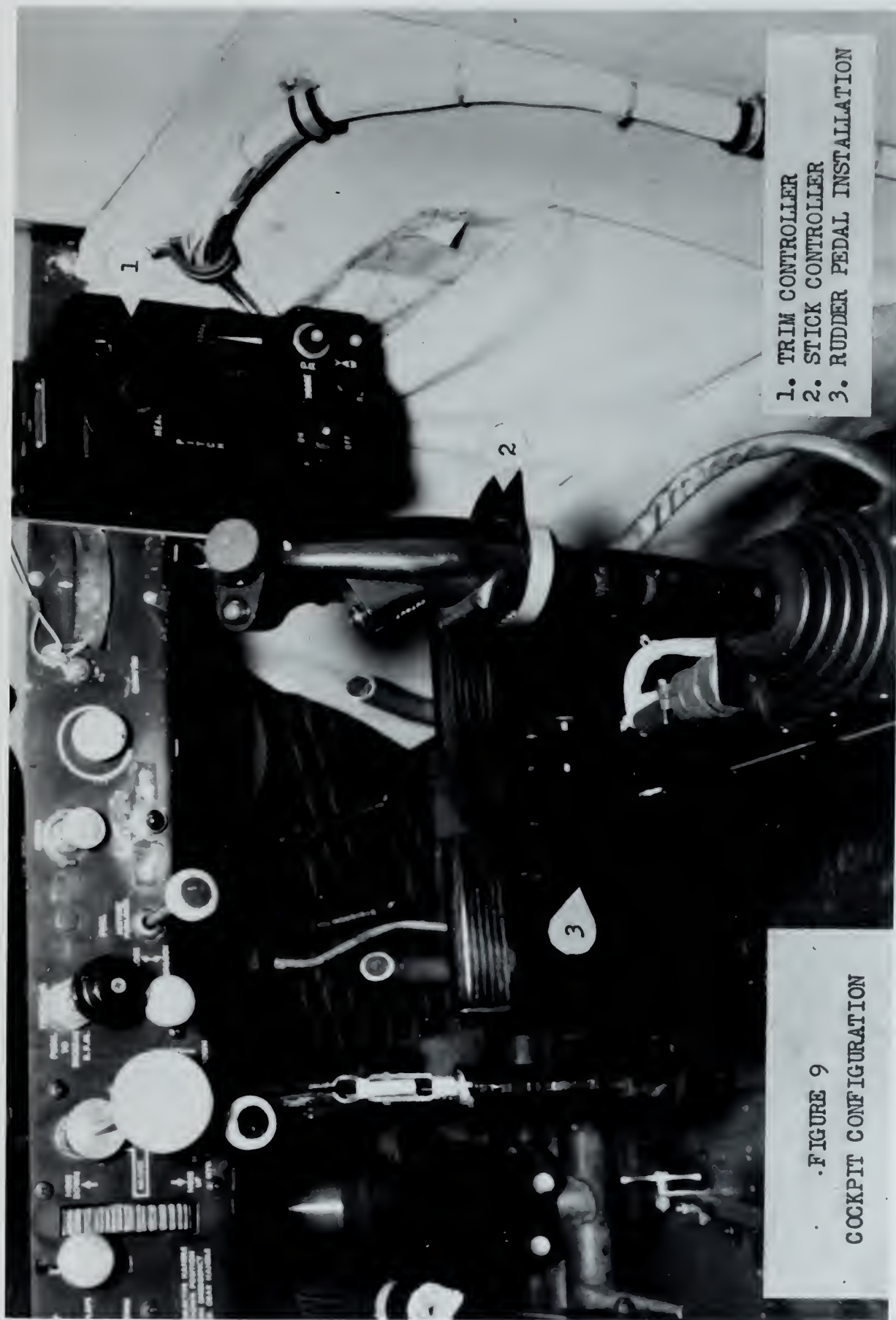
LEGEND

○ PIN NUMBERS
+ TERMINAL STEPS
() GAIN POTENTIOMETERS
GYRO NUMBERS

FIG 8
AUTOPILOT SUMMING CIRCUIT
NAVION



ROLL CHANNEL



1. TRIM CONTROLLER
2. STICK CONTROLLER
3. RUDDER PEDAL INSTALLATION

FIGURE 9
COCKPIT CONFIGURATION

FIGURE 11
 α, β VANE BOOM



1. SIDESLIP VANE
2. ANGLE OF ATTACK VANE

K_4 , DEG RUDDER PER DEG β , $^{\circ}\delta_n/\beta$

0.375

0.250

0.125

0

0.8

0.6

0.4

0.2

GAIN POT SETTING, P_4

FIG 12

GAIN POT SETTING
VERSUS

$^{\circ}\delta_n/\beta$

β FEEDBACK TO YAW CHANNEL

NOTES: 1. RATIO GAIN, P_4 , SET FOR $(^{\circ}\delta_n/\beta)_{MIN}$
2. $^{\circ}\delta_n/\beta = 1.25$
3. EXCITATION VOLTAGE ± 13.5 V

0.2

0.1

0

A.C. VOLTS PER DEG β

0.3

K_B , DEGAUSS PER DEGB, $^{\circ}\delta a/\phi$

1.0 0.5 1.0 1.5

0.8

0.6

0.4

0.2

0.1

0.2

0.3

A.C. VOLTS PER DEGB

(GAIN POT SETTING, P_0)

FIG 13

GAIN POT SETTING

VERSUS

$^{\circ}\delta a/\phi$

β FEEDBACK TO ROLL CHANNEL

NOTES: 1. RATIO GAIN P_0 SET FOR $(80\phi)/\text{MM}$

2. $^{\circ}\delta a/V = 5$

3. EXCITATION VOLTAGE ± 15

1.1

1.2

1.3

1.4

1.5

1.6

1.7

1.8

1.9

2.0

2.1

2.2

2.3

2.4

2.5

2.6

2.7

2.8

2.9

3.0

3.1

3.2

3.3

3.4

3.5

3.6

3.7

3.8

3.9

4.0

4.1

4.2

4.3

4.4

4.5

4.6

4.7

4.8

4.9

5.0

5.1

5.2

5.3

5.4

5.5

5.6

5.7

5.8

5.9

6.0

6.1

6.2

6.3

6.4

6.5

6.6

6.7

6.8

6.9

7.0

7.1

7.2

7.3

7.4

7.5

7.6

7.7

7.8

7.9

8.0

8.1

8.2

8.3

8.4

8.5

8.6

8.7

8.8

8.9

9.0

9.1

9.2

9.3

9.4

9.5

9.6

9.7

9.8

9.9

10.0

10.1

10.2

10.3

10.4

10.5

10.6

10.7

10.8

10.9

11.0

11.1

11.2

11.3

11.4

11.5

11.6

11.7

11.8

11.9

12.0

12.1

12.2

12.3

12.4

12.5

12.6

12.7

12.8

12.9

13.0

13.1

13.2

13.3

13.4

13.5

13.6

13.7

13.8

13.9

14.0

14.1

14.2

14.3

14.4

14.5

14.6

14.7

14.8

14.9

15.0

15.1

15.2

15.3

15.4

15.5

15.6

15.7

15.8

15.9

16.0

16.1

16.2

16.3

16.4

16.5

16.6

16.7

16.8

16.9

17.0

17.1

17.2

17.3

17.4

17.5

17.6

17.7

17.8

17.9

18.0

18.1

18.2

18.3

18.4

18.5

18.6

18.7

18.8

18.9

19.0

19.1

19.2

19.3

19.4

19.5

19.6

19.7

19.8

19.9

20.0

20.1

20.2

20.3

20.4

20.5

20.6

20.7

20.8

20.9

21.0

21.1

21.2

21.3

21.4

21.5

21.6

21.7

21.8

21.9

22.0

22.1

22.2

22.3

22.4

22.5

22.6

22.7

22.8

22.9

23.0

23.1

23.2

23.3

23.4

23.5

23.6

23.7

23.8

23.9

24.0

24.1

24.2

24.3

24.4

24.5

24.6

24.7

24.8

24.9

25.0

25.1

25.2

25.3

25.4

25.5

25.6

25.7

25.8

25.9

26.0

26.1

26.2

26.3

26.4

26.5

26.6

26.7

26.8

26.9

27.0

27.1

27.2

27.3

27.4

27.5

27.6

27.7

27.8

27.9

28.0

28.1

28.2

28.3

28.4

28.5

28.6

28.7

28.8

28.9

29.0

29.1

29.2

29.3

29.4

29.5

29.6

29.7

29.8

29.9

30.0

30.1

30.2

30.3

30.4

30.5

30.6

30.7

30.8

30.9

31.0

31.1

31.2

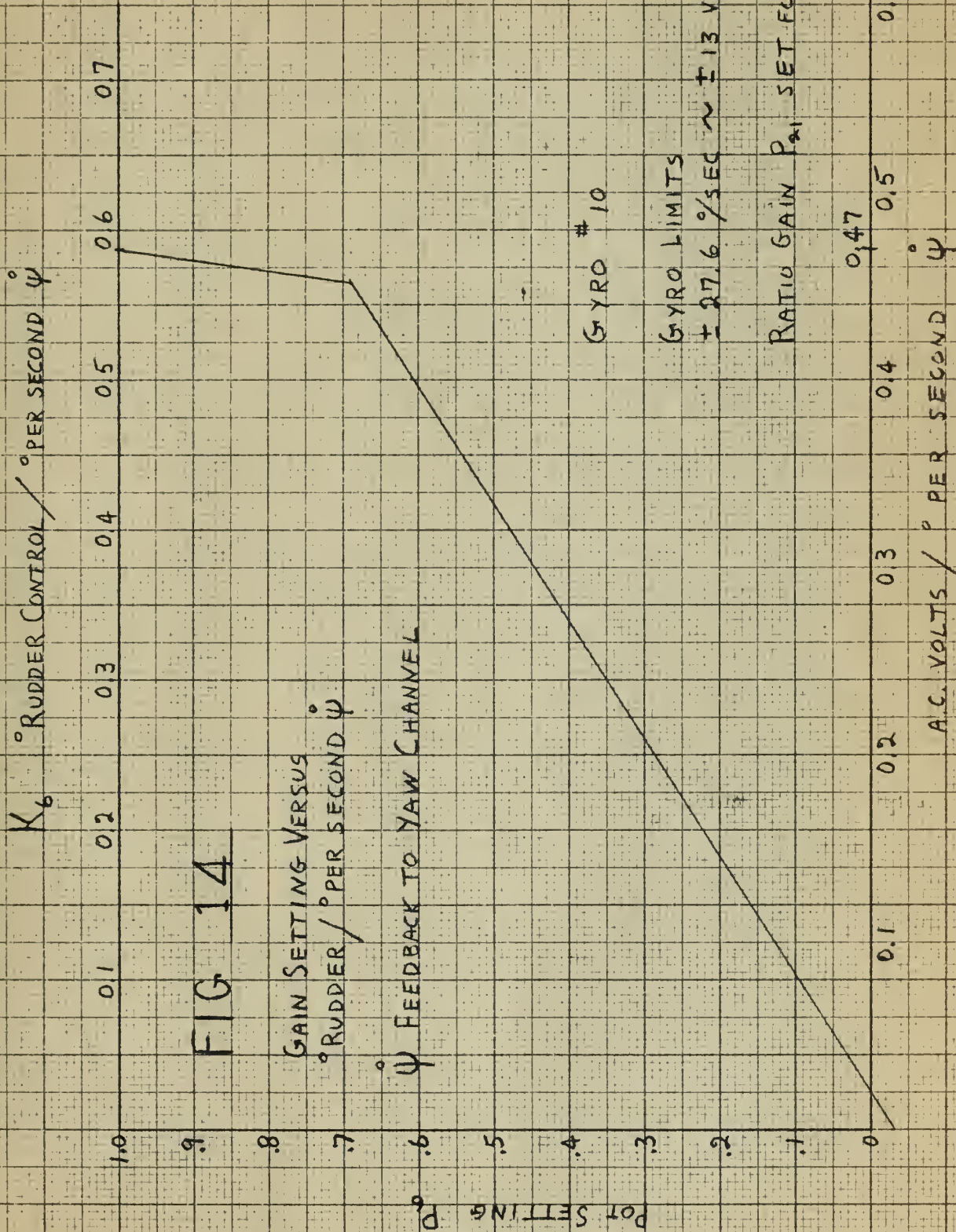
31.3

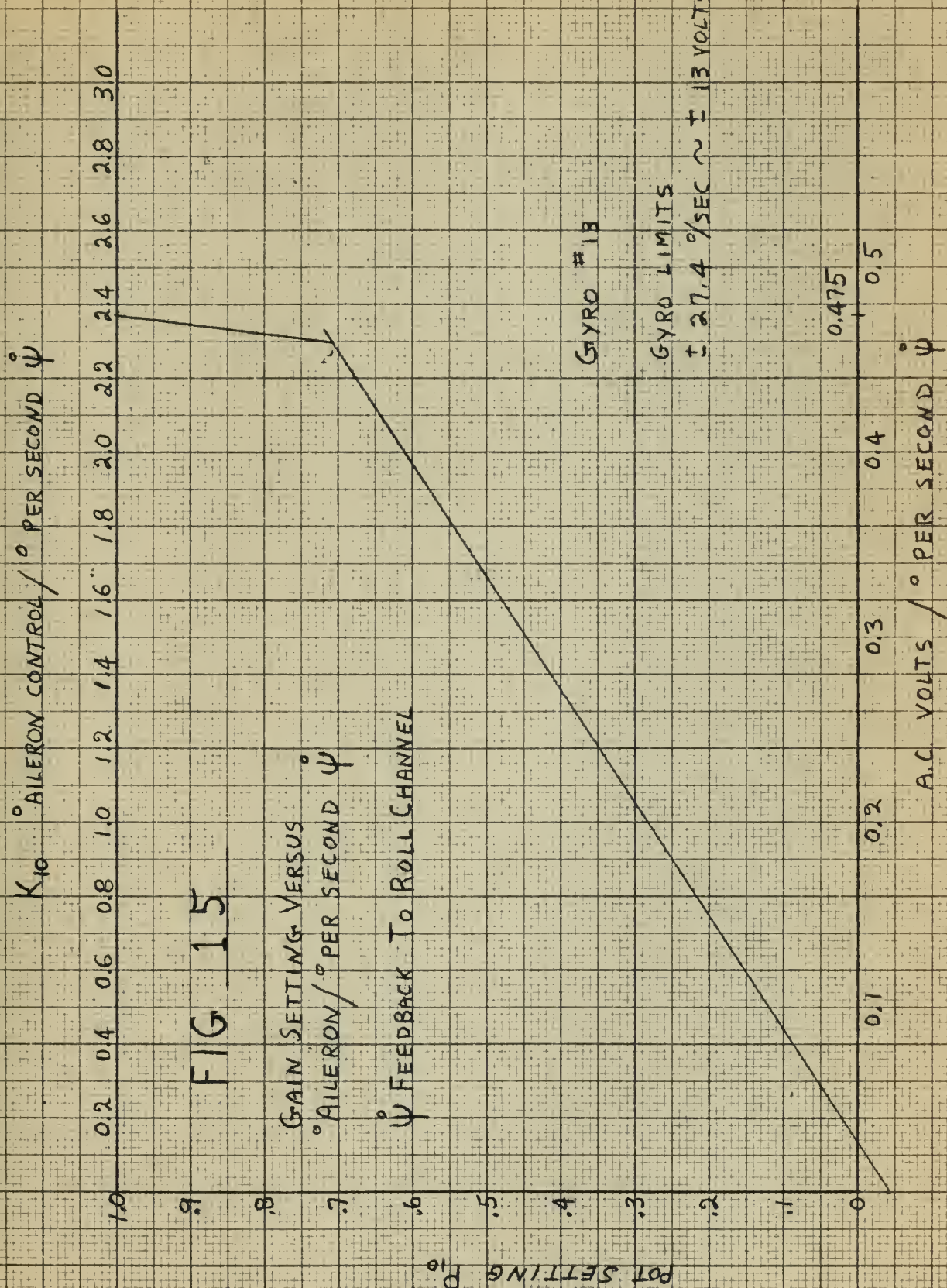
31.4

31.5

31.6

31.7





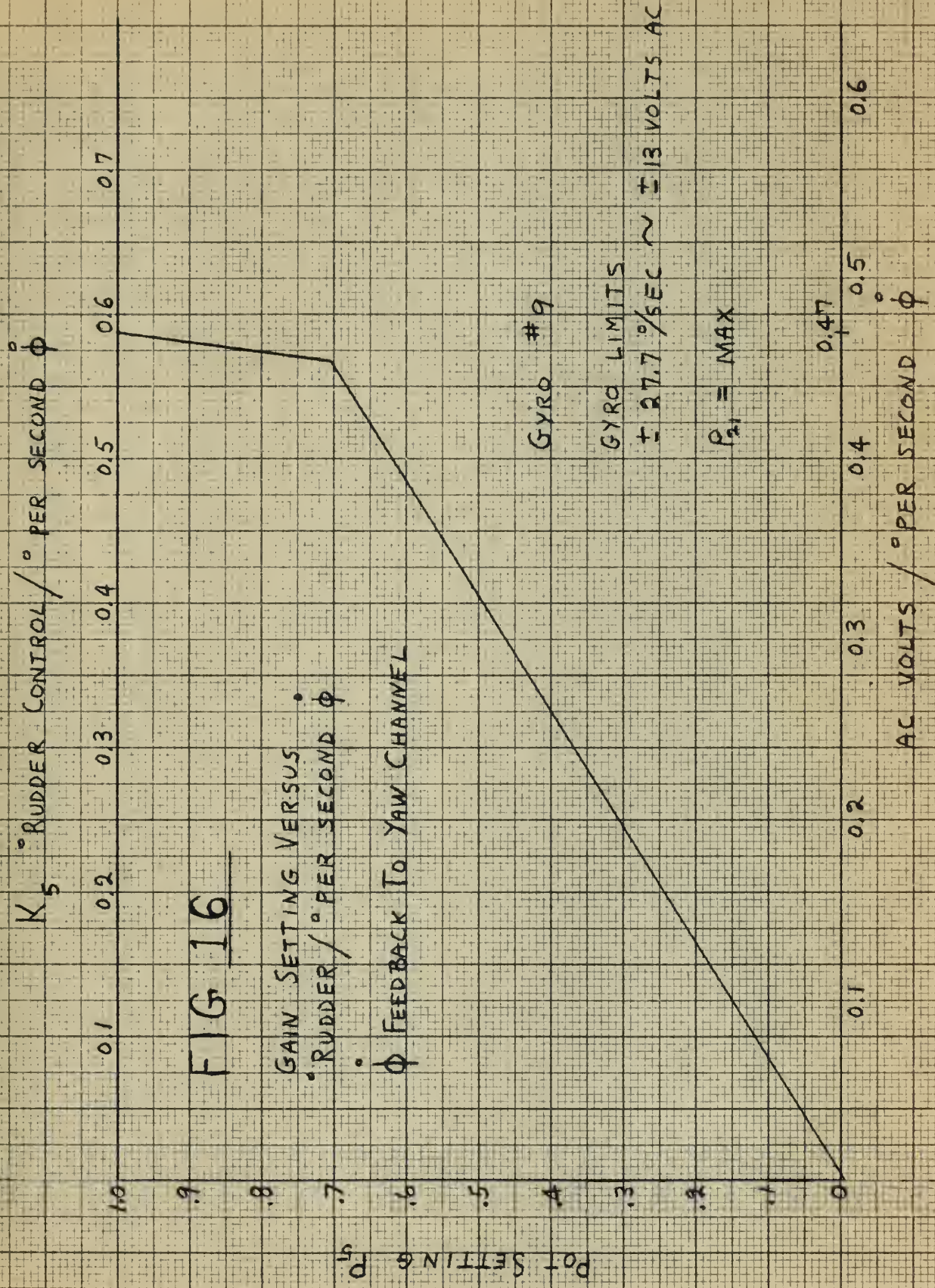
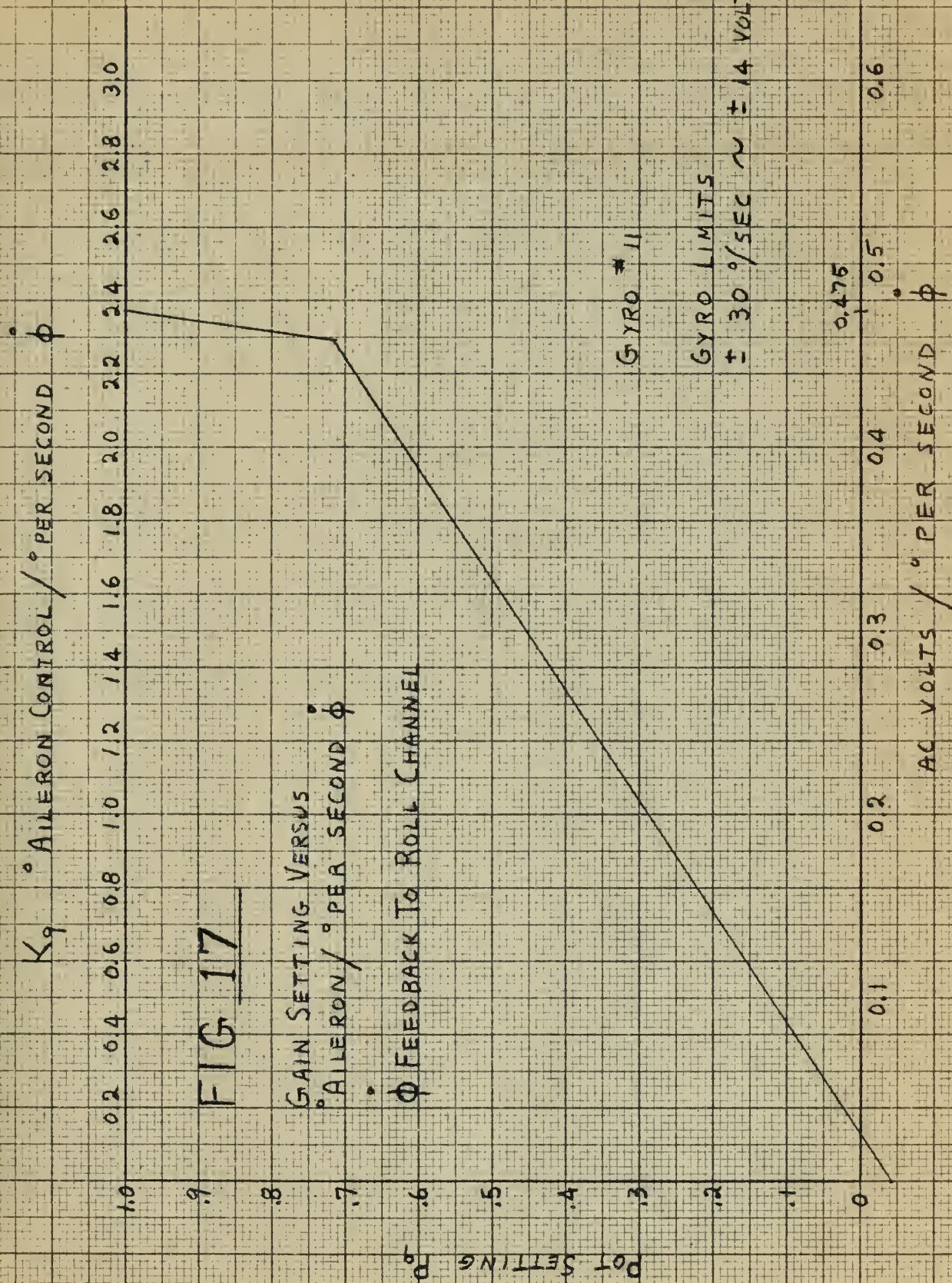


FIG 16

GAIN SETTING VERSUS
 • RUDDER / ° PER SECOND ϕ
 • ϕ FEEDBACK TO YAW CHANNEL



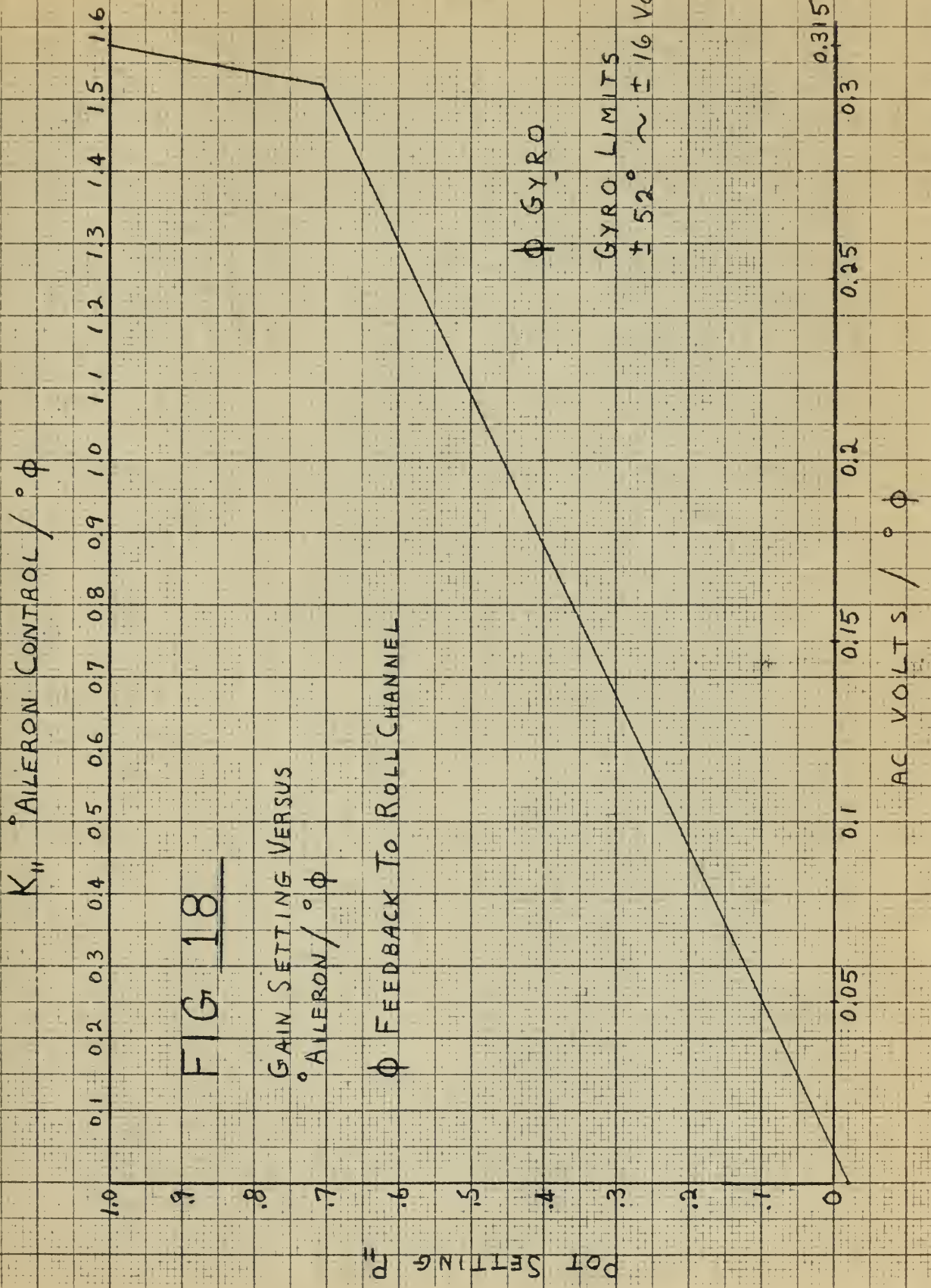


FIG 18

GAIN SETTING VERSUS
°AILERON / ° ϕ

° ϕ FEEDBACK TO ROLL CHANNEL

° GYRO

GYRO LIMITS
 $\pm 52^\circ \sim \pm 16$ VOLTS

° RUDDER DEFLECTION PER VOLT

10
9
8
7
6
5
4
3
2
1
0

FIG 19

° RUDDER DEFLECTION PER VOLT
VERSUS RATIO ADJUSTMENT SETTING

MAX

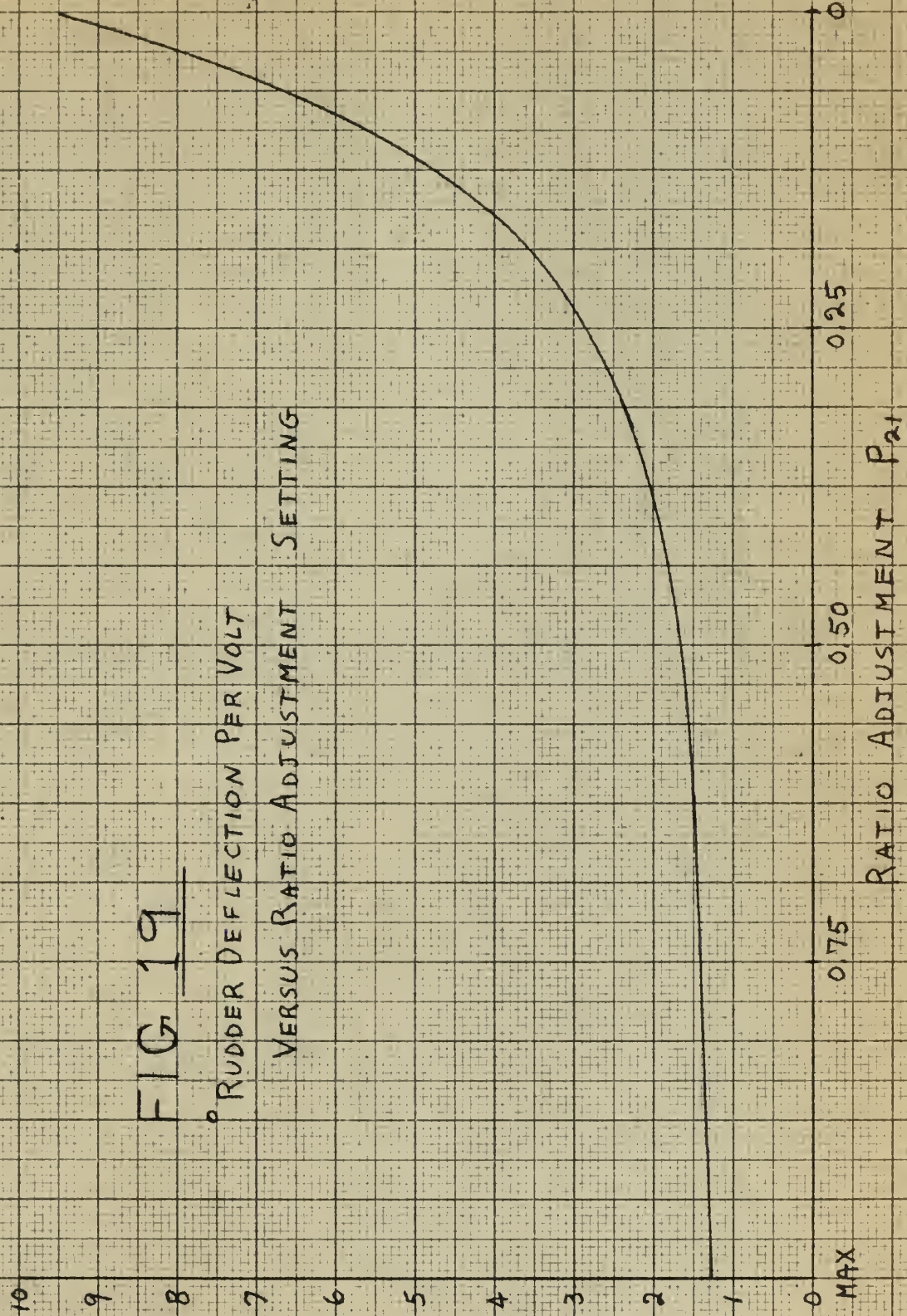
0.75

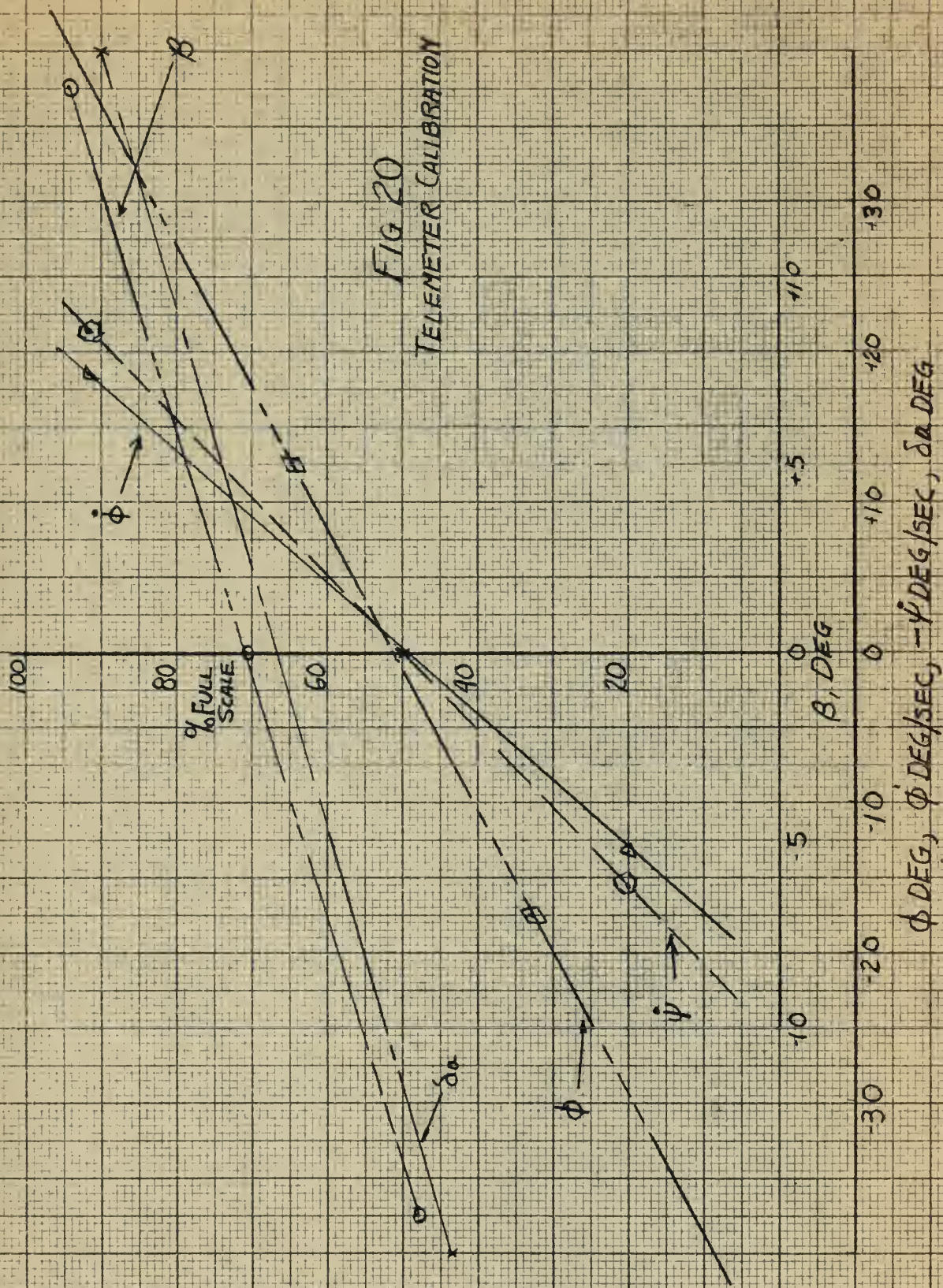
0.50

0.25

0

RATIO ADJUSTMENT P_{21}





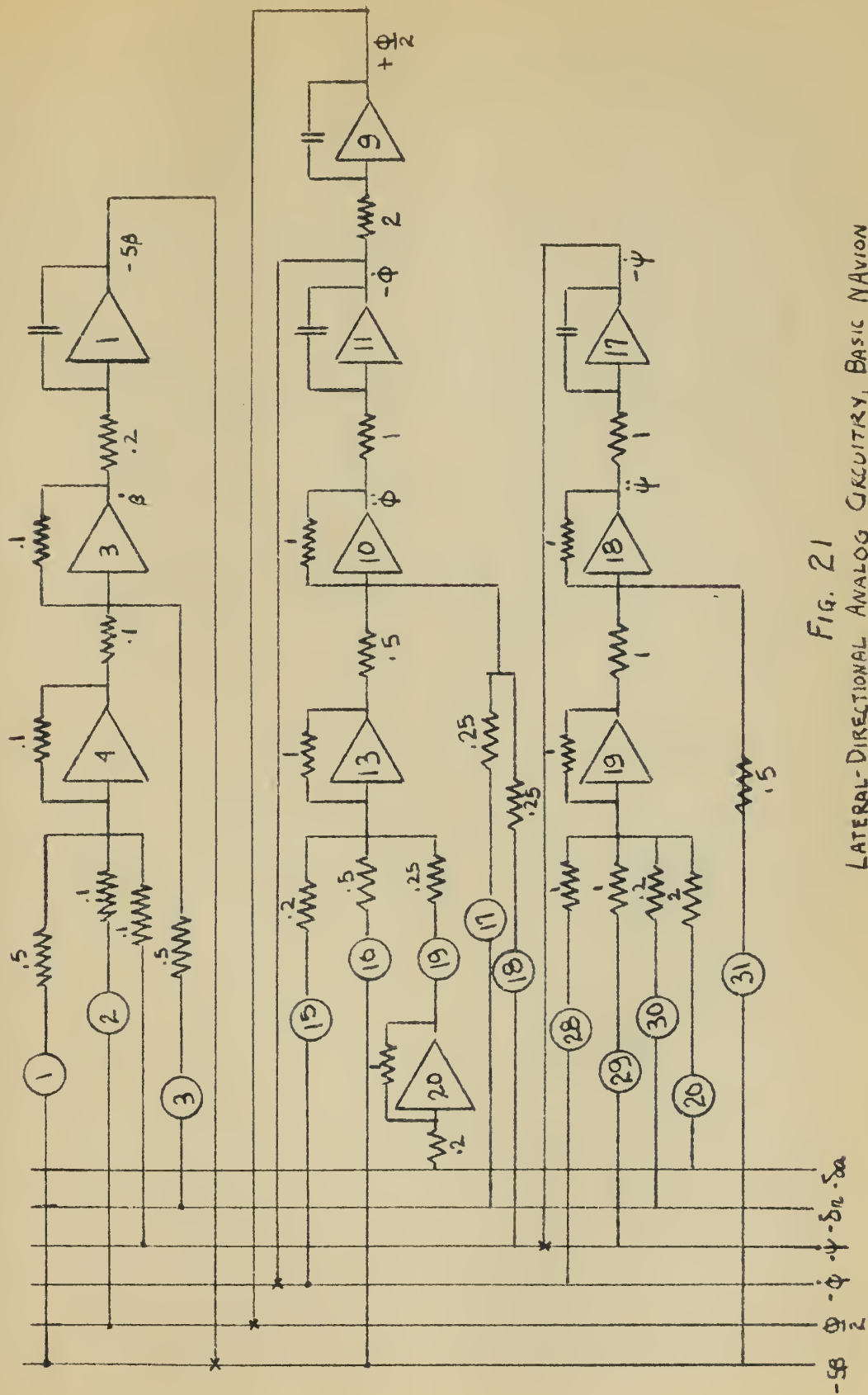


FIG. 21
LATERAL-DIRECTIONAL ANALOG CIRCUITRY, BASIC NAVION

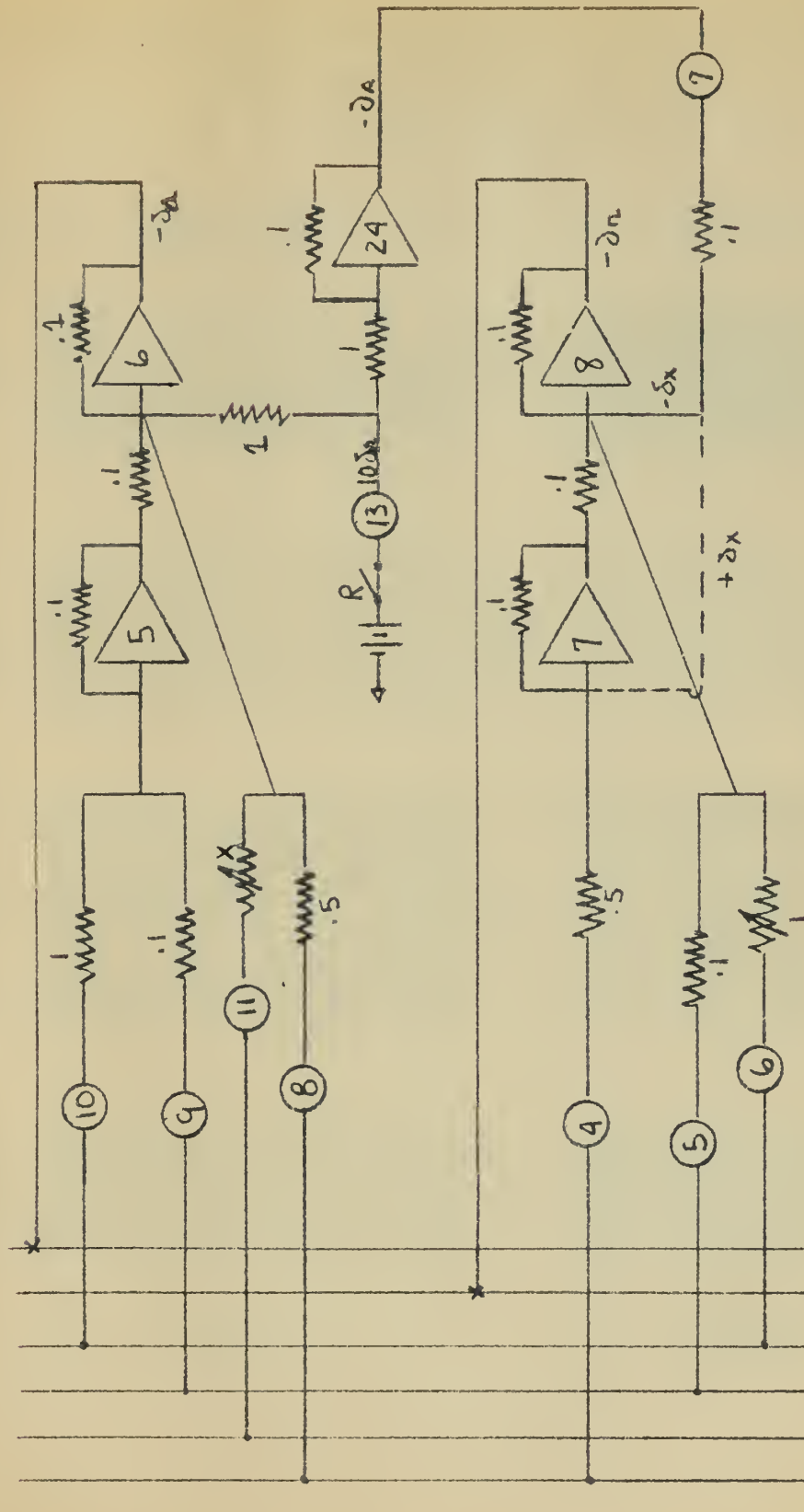


FIG 22
RUDDER ANDAILERON ANALOG CIRCUITRY
"X" AIRPLANE

FIG. 23 RESPONSE TO AILERON STEP FUNCTION BASIC AIRPLANE

ANALOG COMPUTER

FLIGHT TEST

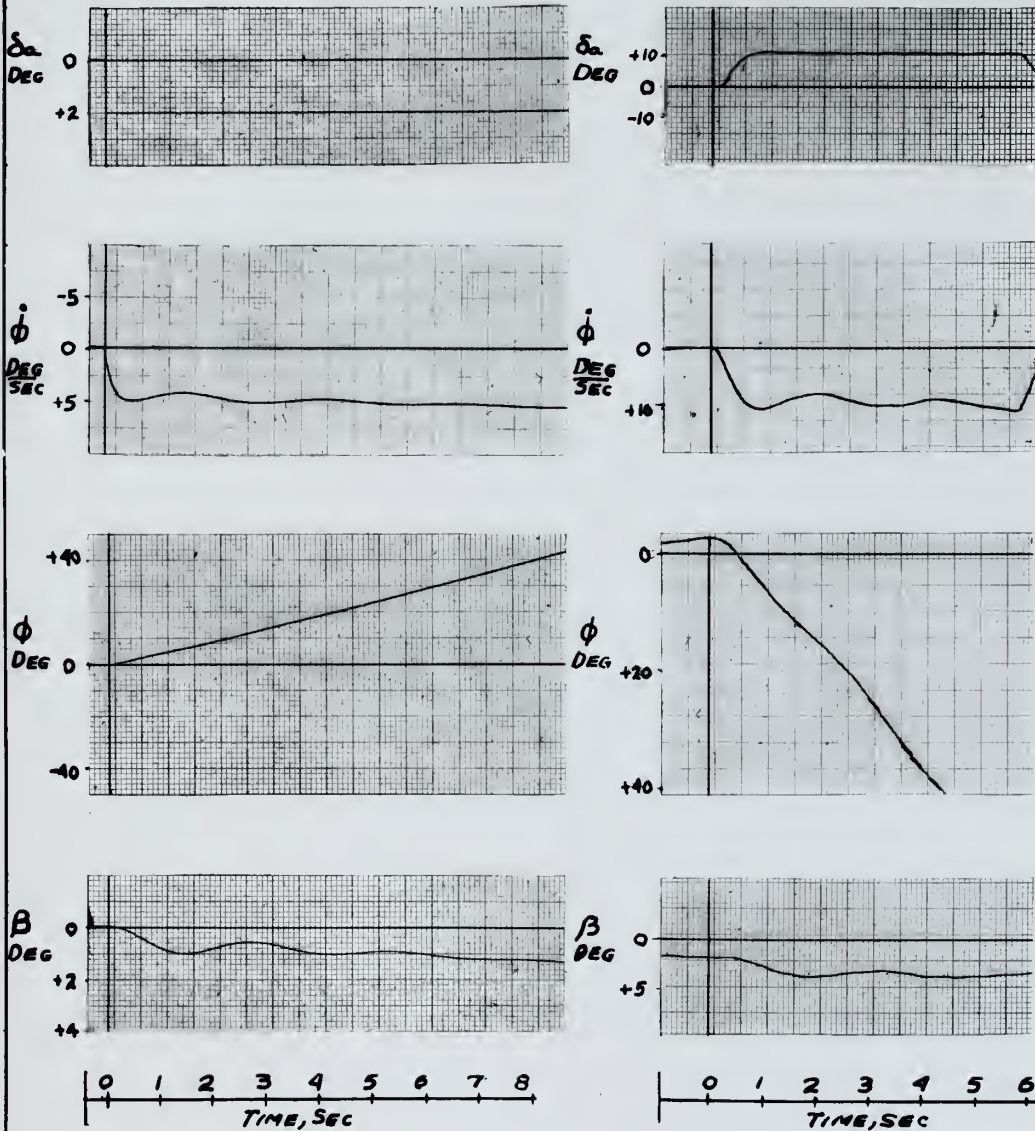


FIG. 24
RESPONSE TO AILERON STEP FUNCTION
"X" AIRPLANE, $\delta_x = 0$

ANALOG COMPUTER

FLIGHT TEST

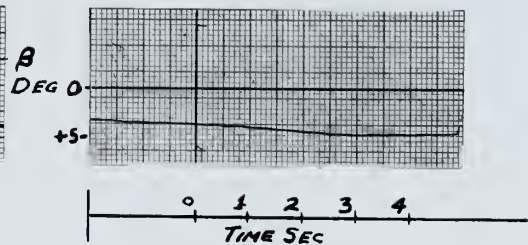
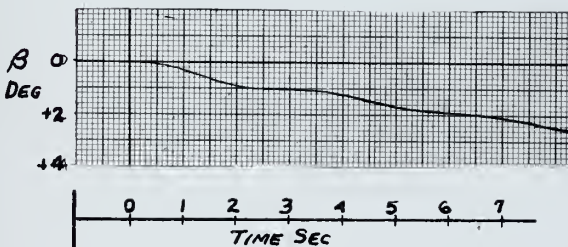
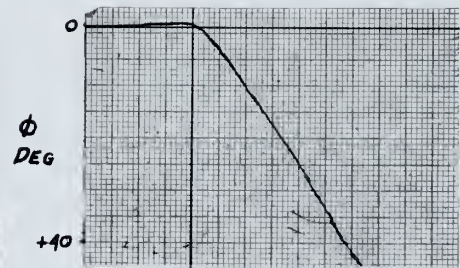
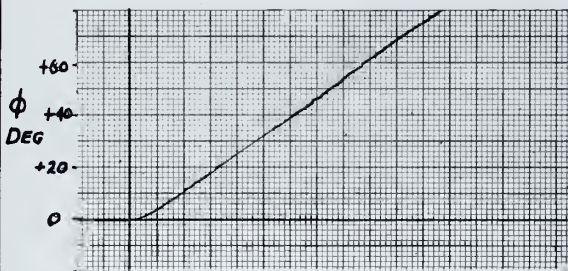
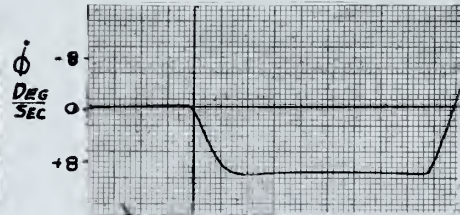
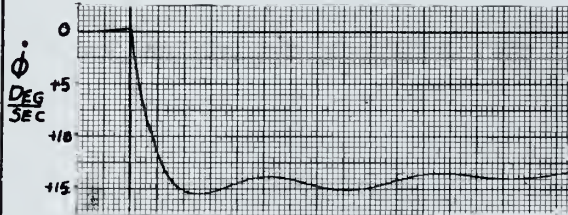
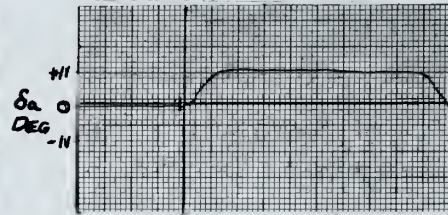
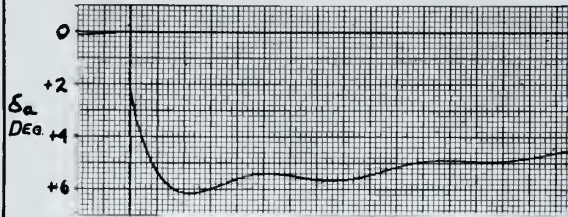
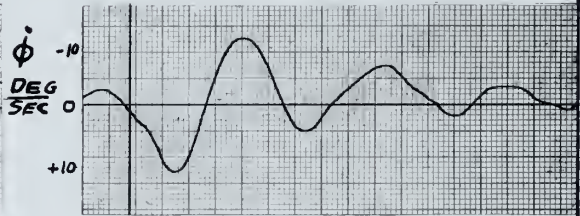
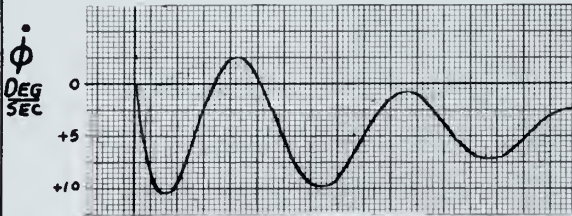
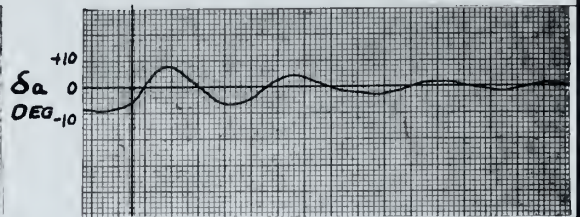
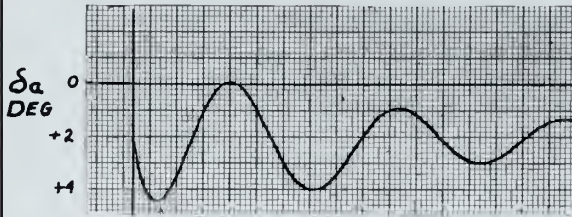


FIG 25 RESPONSE TO AILERON STEP FUNCTION "X" AIRPLANE

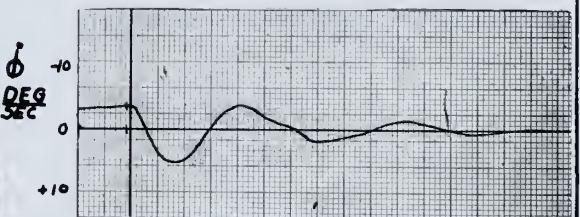
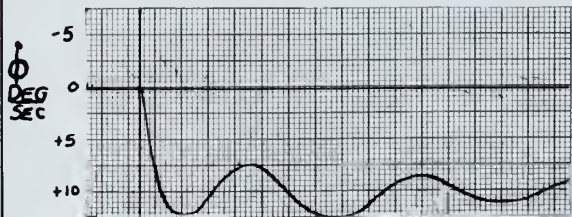
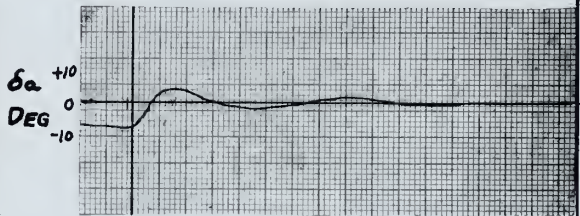
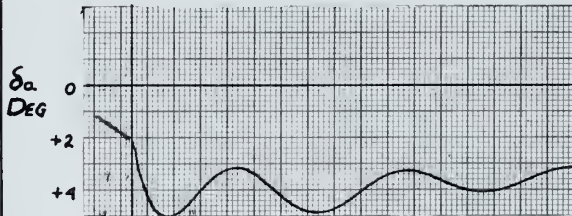
ANALOG COMPUTER

FLIGHT TEST

$$\delta_x = +.915$$



$$\delta_x = +.393$$



0 1 2 3 4 5 6 7
TIME, SEC

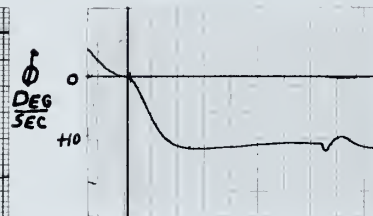
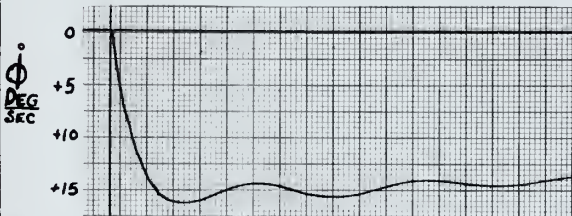
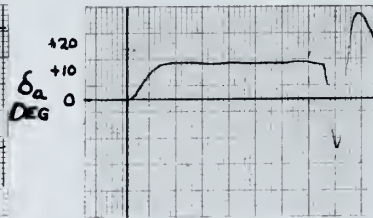
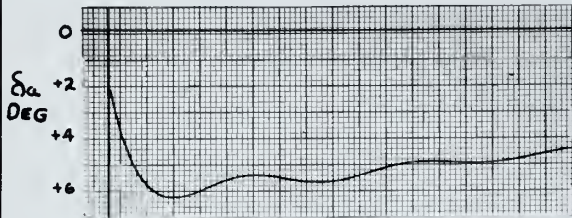
0 1 2 3 4 5 6 7
TIME, SEC

FIG. 26
RESPONSE TO AILERON STEP FUNCTION
"X" AIRPLANE

ANALOG COMPUTER

FLIGHT TEST

$$\delta_x = -.0492$$



$$\delta_x = -.542$$

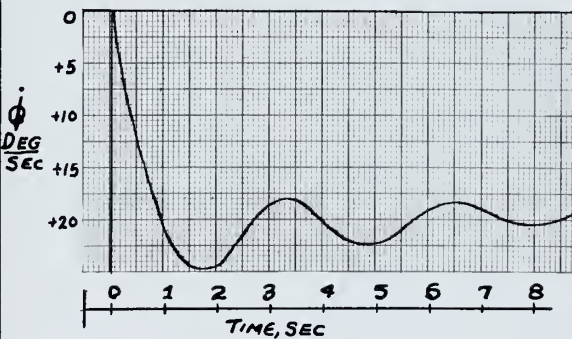
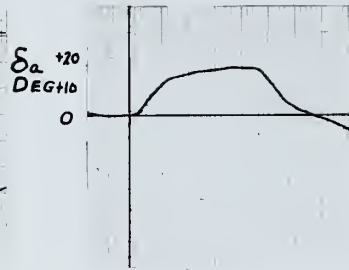
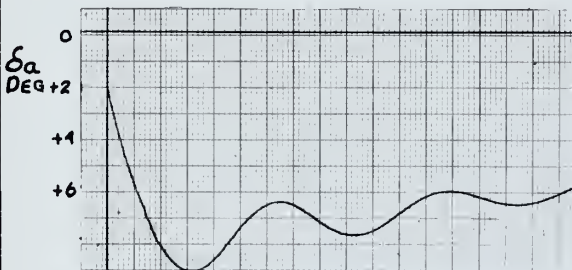
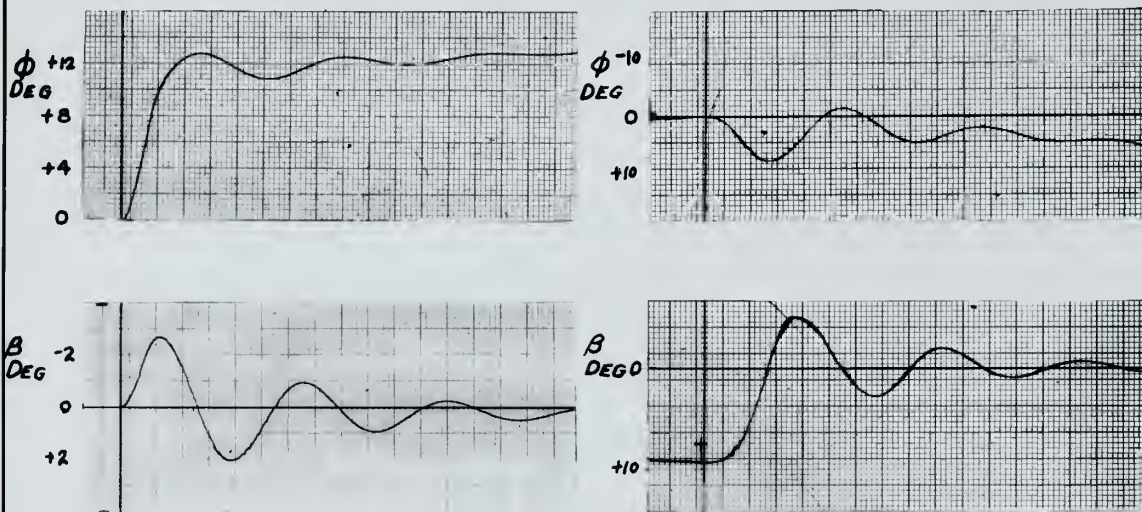


FIG. 27
DUTCH ROLL RESPONSE

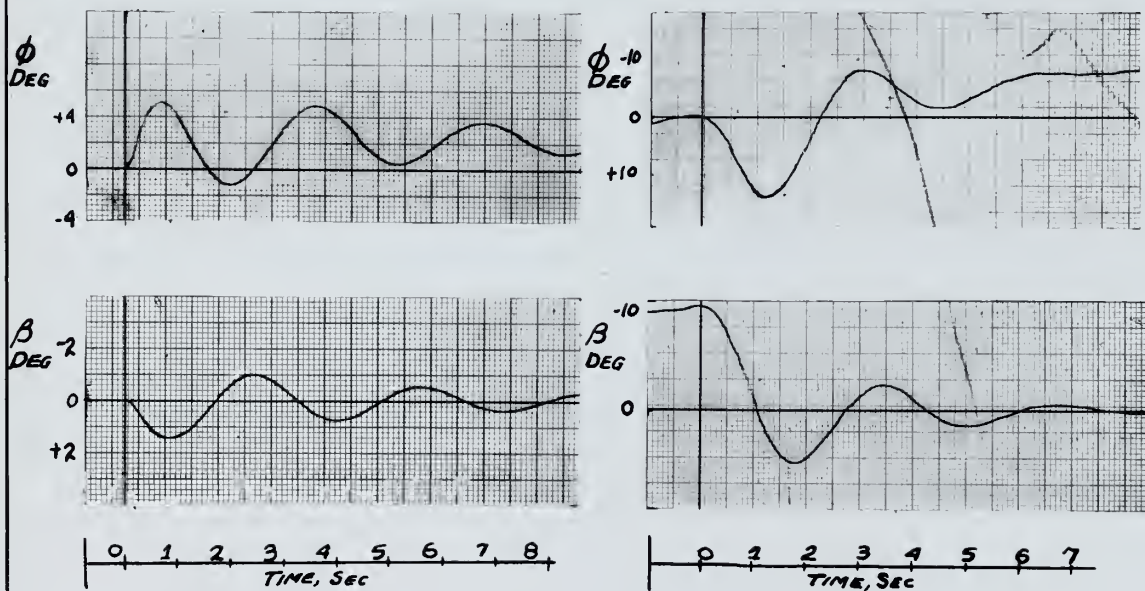
ANALOG COMPUTER

FLIGHT TEST

BASIC AIRPLANE



"X" AIRPLANE



REFERENCES

1. Wiltsie, R.E., and Zink, S.T.: Flight Simulation of the Longitudinal Motions of Another Aircraft. Princeton University Aeronautical Engineering Report No. 508, 1960.
2. Ashkenas, Irving L., and McRuer, Duane T.: The Determination of Lateral Handling Quality Requirements From Airframe-Human Pilot System Studies. WADC Technical Report 59-135, June 1959.
3. Crone, R.M., and A'Harrah, R.C.: Development of Lateral-Directional Flying Qualities Criteria for Supersonic Vehicles, Based on a Stationary Flight Simulator Study. IAS Paper No. 60-18, January 1960.
4. Ashkenas, Irving L., and McRuer, Duane T.: Approximate Airframe Transfer Functions and Application to Single Sensor Control Systems. WADC Technical Report 58-82, June 1958.
5. Perkins, Courtland D., and Hage, Robert E.: Airplane Performance Stability and Control. John Wiley and Sons, New York, 1949.
6. Adams, R.C., Cooper, C.R., and Dedman, T.F.: An Investigation of the Feasibility of Obtaining Lateral Stability Derivatives by Matching Analog Computer Transient Responses to Flight Test Data. Princeton University Aeronautical Engineering Report No. 384, 1957.
7. DeLong, George E., and Moore, Robert S.: The Determination of Lateral Stability Derivatives for a NAVion Airplane from Steady State Dynamic Flight Testing. Princeton University Aeronautical Engineering Report No. 388, May, 1957.
8. Lateral Dynamic Handling Quality Test Program. Cornell Aeronautical Laboratory TM-24.
9. Gowin, Norman E.: Lateral Stability Investigation of an F-100A Airplane. WADC Technical Report 57-563, November 1957.
10. Northrop Aircraft, Inc.: Method of Analysis and Synthesis of Piloted Aircraft Flight Control Systems. BUAER Report AE-61-4-I, March, 1952.
11. Creer, Brent Y., et al: A Pilot Opinion Study of Lateral Control Requirements for Fighter-Type Aircraft. NASA MEMO 1-29-59A, March, 1959.

APPENDIX A

NUMERICAL EVALUATION OF GAIN CONSTANTS

FOR SIMULATION OF THE "X" AIRPLANE

The suggested response specifications for the "X" airplane were:

$$T_R = 0.4 \text{ sec.} \quad \frac{1}{T_S} < \frac{.08}{\text{sec.}} \quad \omega_d \doteq 2 \text{ rad./sec.} \quad \zeta_d = .05$$

$$\left| \frac{\phi}{\beta} \right| \doteq 3 \quad L_{\delta_a} \left(\frac{\omega_\phi}{\omega_d} \right)^2 \sim \text{"good" region from pilot opinion}$$

Longitudinal characteristics \sim "good":

Satisfaction of the requirement on $L_{\delta_a} \left(\frac{\omega_\phi}{\omega_d} \right)^2$ and longitudinal characteristics were accomplished by adjustment of the gain controls for the stick controller to levels satisfactory to the pilot.

Determination of equivalent stability derivatives to satisfy the remaining conditions was based on approximations and associated validity conditions given by Ref. 8. These approximations are based on the following expression for the conventional factorization of the lateral-directional characteristic equation:

$$\begin{aligned} \Delta(s) &= as^4 + bs^3 + cs^2 + ds + e \\ &= \left(s \pm \frac{1}{T_S} \right) \left(s + \frac{1}{T_R} \right) (s^2 + 2\zeta_d \omega_d s + \omega_d^2) \end{aligned}$$

DETERMINATION OF EQUIVALENT STABILITY DERIVATIVES

From $T_R = 0.4$ and $\omega_d = 2$

$$\frac{1}{T_R} \doteq \frac{d}{\omega_d^2} = 2.5$$

$$d = 10$$

$$c \doteq N_{\beta}'' \doteq \omega_d^2 \doteq 4.0$$

$$\text{From } \frac{1}{T_s} < .08$$

$$\frac{1}{T_s} \doteq \frac{e T_R}{\omega_d^2} = 0.1 \quad e < 0.8$$

$$\text{From } \gamma_d = .05$$

$$b \doteq 2 \gamma_d \omega_d + \frac{1}{T_R} = 2.7$$

$$\text{From } \left| \frac{\phi}{\beta} \right| \doteq - \frac{L_\beta''}{N_\beta''} \left[\frac{1}{1 + \frac{1}{\omega_d^2 T_R^2}} \right]^{\frac{1}{2}} \doteq 3 \quad L_\beta'' = -19.25$$

The following solutions for the coefficients of the characteristic equations are based on the complete expansion of Equation (10).

$$\text{From } e < 0.8$$

$$e = \frac{g}{U_0} N_\beta'' \left[\frac{L_\beta'' N_r''}{N_\beta''} - L_r'' \right] + N_\beta'' (1 - \gamma_r'') \left[-L_\phi'' + \frac{L_\beta''}{N_\beta''} N_\phi'' \right]$$

$$+ \gamma_v'' [L_r'' N_\phi'' - N_r'' L_\phi'']$$

$$\text{Let } e = -0.6$$

$$\text{Let } L_\phi'' = N_\phi'' = 0$$

$$\text{Let } N_r'' = -0.3$$

$$\text{Then } L_r'' = 2.26$$

$$\text{From } b = 2.7$$

$$b = - [N_r'' + Y_v'' + L_p''] = 2.7$$

$$L_p'' = -2.184$$

$$\text{From } d = 10$$

$$d = N_\beta'' \left[-L_p'' + \frac{L_\beta''}{N_\beta''} (N_p'' - \frac{g}{U_0}) \right] + Y_v'' (N_p'' L_r'' - N_r'' L_p'')$$

$$+ L_\phi'' (Y_v'' + N_r'') - L_r'' N_\phi''$$

$$N_p'' = 0.122$$

Determination of c

$$c = \left[\frac{L_p''}{N_\beta''} - (N_r'' + Y_v'') + 1 \right] N_\beta'' - N_p'' L_r'' = 4.86$$

The results of these calculations for the equivalent stability derivatives and coefficients of the characteristic equation may be summarized as follows:

$Y_V = -0.216$	$L_R'' = 2.26$	$a = 1$
$g/U_O = 0.183$	$N_\phi'' = 4.0$	$b = 2.7$
$L_\phi'' = -19.25$	$N_P'' = 0.122$	$c = 4.86$
$L_P'' = -2.184$	$N_R'' = -0.30$	$d = 10.0$
$L_\phi'' = 0$	$N_\phi'' = 0$	$e = -0.6$

The approximations used in obtaining these results are subject to the following validity conditions. The degree to which these conditions are satisfied are indicated:

<u>Validity Condition</u>	<u>Degree of Validity</u>
(1) $Y_R'' \doteq Y_P'' \doteq 0$	These conditions assumed
(2) $\left \frac{g}{U_O} \sin \gamma_o \right \ll L_P'' $	γ_o assumed zero
(3) $ Y_V'' N_R'' - N_P'' L_R'' \ll N_\phi''$	$.211 \ll 2$
(4) $ Y_V'' L_R'' \ll L_\phi'' $	$.488 \ll 19.25 $
(5) $\left \frac{L_P''}{N_\phi''} (Y_V'' + N_R'') \right \ll 1$	$.308 \ll 1$
(6) $\left \frac{L_\phi''}{L_P'' N_\phi''} (N_P'' - g/U_O) \right \ll 1$	$.1341 \ll 1$
(7) $\gamma_d < 0.2$	$\gamma_d \doteq .05$

The degree of validity shown in satisfying condition (5) is marginal. The importance of satisfying this condition, which is one of the validity conditions in the dutch roll damping approximation, was seen by applying the condition to the basic NAVION derivatives. For this case the validity condition was not satisfied and the resultant approximation for $2 \gamma_d \omega_d$ was a negative value.

Variation of the $\frac{\omega_\phi}{\omega_a}$ ratio was accomplished by artificial variation of the control derivative ratio $\frac{N_{\delta_a}''}{L_{\delta_a}''}$ assuming no rudder deflection due to rudder pedal input. Variation of this ratio is described by the following equation:

$$\frac{N_{\delta_a}''}{L_{\delta_a}''} = \frac{N_{\delta_a} + N_{\delta_r} \delta_x}{L_{\delta_a} + L_{\delta_r} \delta_x} \quad \text{where} \quad \frac{K_7}{K_{13}} \equiv \delta_x$$

Numerical evaluation of the required values for the K_1 and for the K_7/K_{13} ratio required for the range of the $\frac{\omega_\phi}{\omega_a}$ ratio was accomplished by utilization of the numerical formulae listed in Table IV, with the following results:

<u>K_1</u>	<u>Numerical Value</u>	<u>$\frac{\omega_\phi}{\omega_a}$</u>	<u>$\frac{N_{\delta_a}''}{L_{\delta_a}''}$</u>	<u>δ_x</u>
K_4	0.248	0.5	- 0.156	0.915
K_5	- 0.152	0.8	- 0.075	0.393
K_6	- 0.046	1.0	0	- 0.0492
K_8	- 0.484	1.2	0.092	- 0.542
K_9	0.271			
K_{10}	0.020			
K_{11}	0			

thesE148

A preliminary evaluation of the NAVion a



3 2768 001 90289 3

DUDLEY KNOX LIBRARY